Eidgenössische Technische Hochschule Zürich
Swiss Federal Institute of Technology Zurich

Seminar for Applied Mathematics SAM

hp-FEM for reaction-diffusion equations. II: Robust exponential convergence for multiple length scales in corner domains

L. Banjai and J.M. Melenk and Ch. Schwab

Research Report No. 2020-28
May 2020

Seminar für Angewandte Mathematik
Eidgenössische Technische Hochschule
CH-8092 Zürich
Switzerland

Funding: Austrian Science Fund (FWF) project F 65; Swiss National Science Foundation.

HP-FEM FOR REACTION-DIFFUSION EQUATIONS II. ROBUST EXPONENTIAL CONVERGENCE FOR MULTIPLE LENGTH SCALES IN CORNER DOMAINS. *

LEHEL BANJAI†, JENS M. MELENK‡, AND CHRISTOPH SCHWAB§

Abstract. In bounded, polygonal domains $\Omega \subset \mathbb{R}^2$ with Lipschitz boundary $\partial\Omega$ consisting of a finite number of Jordan curves admitting analytic parametrizations, we analyze hp-FEM discretizations of a linear, second order, singularly perturbed reaction diffusion equations on so-called geometric boundary layer meshes. We prove, under suitable analyticity assumptions on the data, that these hp-FEM afford exponential convergence, in the natural "energy" norm of the problem, as long as the geometric boundary layer mesh can resolve the smallest length scale present in the problem. Numerical experiments confirm the exponential convergence.

Key words. anisotropic hp–refinement, geometric corner refinement, exponential convergence.

AMS subject classifications. 65N12, 65N30.

1. Introduction. The need for accurate numerical approximations of solutions to singularly perturbed partial differential equations in nonsmooth domains arises in a wide range of applications. Higher order numerical methods must cope with the appearance of boundary layers and their interaction with geometric corner and edge singularities. They are due to length scales introduced into weak solutions by small or large parameters in the differential operator. Accordingly, a large body of numerical analysis research has been developed during the past decades on their efficient numerical resolution; we mention only [21, 23] and the references there for reaction-advection-diffusion problems, and [27] for viscous, incompressible flow. The discretization methods presented and surveyed in [23] are of fixed order and of Finite Difference or Finite Element type. They account specifically for the appearance of boundary and interior layers in solutions of the singularly perturbed boundary value problems. Being of fixed order, the corresponding discretization methods can afford at best fixed, algebraic orders of convergence whose convergence is, however, robust: the constants implicit in *a priori* error bounds are independent of the singular perturbation parameters and, hence, of the physical length scales in solutions that are implied by the singular perturbation of the governing equations.

As it is well-known, elliptic boundary value problems in domains Ω with piecewise analytic boundary for differential operators with analytic in $\overline{\Omega}$ coefficients and forcing terms admit exponential convergence rates by Galerkin approximations with local mesh refinement and concurrent, judicious increase of the polynomial degree. This so-called hp-Finite Element approach has been analyzed in a series of papers, see [5,29] and, more recently, in [25,26,28], and the references there, for regular elliptic boundary value problems.

* The research of JMM was supported by the Austrian Science Fund (FWF) project F 65. Work performed in part while CS was visiting the Erwin Schrödinger Institute (ESI) in Vienna in June-August 2018 during the ESI thematic period "Numerical Analysis of Complex PDE Models in the Sciences". Research of CS supported in part by the Swiss National Science Foundation.

†Maxwell Institute for Mathematical Sciences, School of Mathematical & Computer Sciences, Heriot-Watt University, Edinburgh EH14 4AS, UK (l.banjai@hw.ac.uk).

‡Institut für Analysis und Scientific Computing, Technische Universität Wien, A-1040 Vienna, Austria (melenk@tuwien.ac.at).

§Seminar for Applied Mathematics, ETH Zürich, ETH Zentrum, HG G57.1, CH8092 Zürich, Switzerland (christoph.schwab@sam.math.ethz.ch).

The study of parametric regularity and proof of robust, algebraic convergence rates of discretizations for singularly perturbed, elliptic boundary value problems on polygons seems to have been initiated by G.I. Shiskhin in the 1980s [32].

For singular perturbation problems, corresponding results on robust exponential convergence rates and corresponding analytic regularity estimates for solutions have been obtained in a series of papers in the 1990s, see [15, 16, 18, 19] and the references there. The results from [15, 16, 19] were restricted to domains Ω with smooth (analytic) boundary $\partial\Omega$. In [20] analytic regularity results for elliptic reaction-diffusion problems in two space dimensions that are uniform with respect to the perturbation parameter were obtained. These results allowed us in [19] to prove robust exponential convergence of hp-FEM with so-called two-element and geometric boundary layer meshes, in domains Ω with a smooth (analytic) boundary $\partial\Omega$. In [18], an analytic regularity theory for solutions of linear, singularly perturbed elliptic reaction-diffusion problems in polygonal domains Ω as depicted in Fig. 1.1 was developed. In these works, elliptic singular perturbations with exactly one small length scale were considered. Examples of elliptic singular perturbation problems where several characteristic length scales appear simultaneously comprise in particular dimensionally reduced models of curved thin solids ("shells") in so-called "bending-dominated" states (see, e.g., [9] and the references there for a detailed discussion of possible length scales), and linear, elliptic reaction-diffusion boundary value problems that result from implicit time-discretizations of parabolic evolution equations and, more recently, from discretizations of fractional powers of elliptic operators (see, e.g., [6, 17] and the references there). Further applications of the presently developed results arise in electromagnetics in so-called eddy-current models (where the small parameter is a complex number) (see, e.g., [8] and the references there), and in hp-FEM for advection-diffusion problems where stability, in addition to consistency, is a major issue (see, e.g., [10, 16]).

The present work extends in the reaction-diffusion case the hp-error analysis of Part I [19] to polygons and addresses the question how to approximate problems with multiple scales. The meshes presented here are also appropriate in situations where the precise length scales are unavailable, as is the case for example in problems from computational mechanics, see, e.g. [9]. We next present a model singularly perturbed linear elliptic diffusion problem, where the perturbation parameter $0 < \varepsilon \leq 1$ dictates the single boundary length scale ε. We hasten to add that the ensuing hp-approximation results hold, independent of the particular model problem, and apply to a wider range of singular perturbations, as plate and shell models with possibly multiple length scales. See, e.g., [2, 9, 12, 13] and the references there.

1.1. Model reaction-diffusion problem. In a bounded domain $\Omega \subset \mathbb{R}^2$, which is assumed to be scaled to unit size, and for a parameter $0 < \varepsilon \leq 1$, we consider the hp-FE approximation of the model reaction-diffusion Dirichlet problem

$$-\varepsilon^2 \nabla \cdot (A(\mathbf{x})\nabla u_\varepsilon) + c(\mathbf{x}) u_\varepsilon = f \quad \text{in } \Omega, \qquad u_\varepsilon = 0 \quad \text{on } \partial\Omega. \tag{1.1}$$

We assume

$$\begin{aligned} &A,\ c,\ f \text{ analytic on } \overline{\Omega}, \text{ independent of } \varepsilon, \\ &A \text{ symmetric, positive definite uniformly in } \overline{\Omega},\ c \geq c_0 > 0 \text{ on } \overline{\Omega}. \end{aligned} \tag{1.2}$$

We again emphasize that we consider (1.1) for illustration. The scope of the robust exponential hp convergence rate bounds below extends well beyond (1.1) to more complex, singularly perturbed PDE such as those in [2, 9, 12].

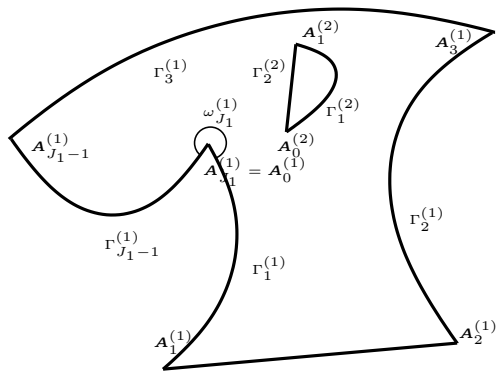

FIG. 1.1. *Example of a curvilinear polygon*

1.2. Geometric Preliminaries. In (1.2), the domain $\Omega \subset \mathbb{R}^2$ is a curvilinear polygonal domain, schematically depicted in Fig. 1.1. Specifically, the boundary $\partial\Omega$ is assumed to consist of $J \in \mathbb{N}$ closed curves $\Gamma^{(i)}$. Each curve $\Gamma^{(i)}$ in turn is assumed to be partitioned into finitely many open, disjoint, analytic arcs $\Gamma_j^{(i)}$, in the sense that there are numbers $J_i \in \mathbb{N}$ such that

$$\overline{\Gamma^{(i)}} = \bigcup_{j=1}^{J_i} \overline{\Gamma_j^{(i)}} \ , \quad i = 1, \ldots, J \ .$$

Here, analytic arcs $\Gamma_j^{(i)}$ admit nondegenerate, analytic parametrizations, i.e.,

$$\Gamma_j^{(i)} = \left\{ \mathbf{x}_j^{(i)}(\theta) | \theta \in (0,1) \right\} \ , \quad i = 1, ..., J, \quad j = 1, ..., J_i \ .$$

with the coordinate functions $x_j^{(i)}$, $y_j^{(i)}$ of $\mathbf{x}_j^{(i)}(\theta) = (x_j^{(i)}(\theta), y_j^{(i)}(\theta))$ assumed to be (real) analytic functions of $\theta \in [0,1]$ and such that

$$\min_{\theta \in [0,1]} \left\{ \left| \frac{d}{d\theta} x_j^{(i)}(\theta) \right|^2 + \left| \frac{d}{d\theta} y_j^{(i)}(\theta) \right|^2 \right\} > 0 \quad j = 1, ..., J_i, \quad i = 1, ..., J \ .$$

We denote $\partial\Gamma_j^{(i)} = \{\boldsymbol{A}_{j-1}^{(i)}, \boldsymbol{A}_j^{(i)}\}$ where $\boldsymbol{A}_{j-1}^{(i)} = \mathbf{x}_j^{(i)}(0)$ and $\boldsymbol{A}_j^{(i)} = \mathbf{x}_j^{(i)}(1)$. For each boundary component $\Gamma^{(i)}$, we enumerate $\{\boldsymbol{A}_j^{(i)}\}_{j=1}^{J_i}$ cyclically, counterclockwise by indexing with j modulo J_i, thereby identifying in particular $\boldsymbol{A}_j^{(i)} := \boldsymbol{A}_{j+J_i}^{(i)}$. The interior angle at $A_j^{(i)}$ is denoted $\omega_j^{(i)} \in (0, 2\pi)$. For notational simplicity, we assume henceforth that $J = 1$, i.e., $\partial\Omega$ consists of a single component of connectedness. We write $\boldsymbol{A}_j = \boldsymbol{A}_j^{(1)}$, Γ_j for $\Gamma_j^{(1)}$, $x_j = x_j^{(1)}$, $y_j = y_j^{(1)}$. Then, in a vicinity of any point $x \in \partial\Omega$, a curvilinear polygon Ω is analytically diffeomorphic to either a half-space, or to a plane sector with vertex situated at the origin.

1.3. Contributions. The principal contribution of the present paper is robust, exponential convergence of a class of *hp*-FEM approximations of the singular perturbation problem (1.1) under the analyticity assumptions (1.2), in curvilinear polygons Ω as described in Section 1.2. The convergence proof in Sections 3 and 4 is done under a scale resolution condition that corresponds, roughly speaking, to the *hp*-FE

partitions resolving the shortest length scale that occurs in the solution u_ε, and it is strongly based on parameter-explicit, analytic regularity results for the parametric solution family $\{u_\varepsilon : 0 < \varepsilon \leq 1\} \subset H^1_0(\Omega)$ of (1.1), which were obtained by one of the authors in [18]. Importantly, and distinct from earlier work on robust exponential *hp*-FE convergence for (1.1), a patch-based convergence proof is developed which also enables an algorithmic, patchwise-structured anisotropic mesh specification, described in Section 2, which is applicable in domains Ω of the generality admitted in Section 1.2. As we show in numerical experiments in Section 5, the recently developed, automatic mesh generator NETGEN [24] does produce automatically, i.e., without "expert pruning", anisotropic, geometric meshes in Ω with the required boundary and corner refinement which satisfy the requirement of the present robust, exponential convergence bounds.

1.4. Outline of this paper. In Section 2, we introduce the geometric mesh families in Ω which underlie our robust exponential convergence results. The meshes require concurrent anisotropic geometric partitions of Ω towards the boundary $\partial\Omega$, and towards the corners $\boldsymbol{A}_j$. We define these meshes in a macro-element fashion based on an initial, coarse regular partition of the physical domain Ω into a macro-triangulation consisting of a regular, finite, and fixed partition of the physical domain Ω which is described in Section 2.1. Its elements will be referred to as (macro) patches and are assumed to be images of a finite number of quadrilateral reference patches under analytic patch maps. The reference patches are key in ensuring robust exponential convergence rate bounds of our *hp*-FEM approximation. Following earlier work [15, 16, 18], we consider so-called geometric boundary layer meshes, denoted by $\mathcal{T}^{L,n}_{geo,\sigma}$. We introduce these in Def. 2.3. Unlike the so-called "two-element" meshes considered earlier in [30, 31], which are designed to approximate only a single small scale in a robust way, the presently considered geometric boundary layer meshes afford robust exponential convergence rates of *hp*-FEM also in the presence of multiple physical length scales. This situation arises in a number of applications (e.g., [6, 9]). Section 2.3 introduces the geometric boundary layer mesh, first on the reference patches, and then in Section 2.4 in curvilinear polygons.

Section 3 is devoted to the polynomial approximation of functions on geometric boundary layer meshes. The approximation is based on Gauss-Lobatto interpolation operators in the reference triangle, indicated by $\triangle$, and in the reference square, indicated by $\square$, in Section 3.1. These are then assembled into (nodal) patch approximation operators on the geometric boundary layer patches in Section 3.2. Then, the robust *hp*-approximation of corner singularities and boundary layer functions is proved. These functions are the key solution components of singularly perturbed problems in polygons such as the model problem (1.1).

Section 4 assembles the patch *hp*-approximation results and interpolants into a global approximation operator, and presents the main result of this paper: robust exponential convergence rate bounds for the global *hp*-interpolation of the solution of (1.1) assembled from the patch approximations.

Section 5 presents several illustrative numerical experiments in polygons, which underline the theoretical results. They are based on *hp*-meshes that are furnished by the automated mesh generation procedure NETGEN [24] to make the point that the somewhat technical construction of geometric boundary layer meshes is, in principle, available and feasible automatically. Appendix A contains proofs of auxiliary results on analytic regularity estimates under analytic changes of variables. Appendix B collects (mostly known) results on univariate polynomial approximation for convenient

reference in the main text.

1.5. Notation. We employ standard notation for Sobolev spaces. Constants C, γ, $b > 0$ may be different in different instances. However, they will be independent of parameters of interest such as $\varepsilon \in (0,1]$ and the polynomial degree q. The notation $\nabla^n u$ stands for the collection of all partial derivatives of order n and $|\nabla^n u|^2 = \sum_{|\alpha|=n} \frac{n!}{\alpha!}|D^\alpha u|^2$. Points in $\mathbb{R}^2$ will be denoted depending on the context as either $\mathbf{x} = (x,y)$ (physical domain) or $\widetilde{\mathbf{x}} = (\widetilde{x},\widetilde{y})$ (patch domains) or $\widehat{\mathbf{x}} = (\widehat{x},\widehat{y})$ (reference domains). We abbreviate $\{\widetilde{x}=0\}$, $\{\widetilde{y}=0\}$, and $\{\widetilde{x}=\widetilde{y}\}$ for the line segments $\{\widetilde{\mathbf{x}} = (0,\widetilde{y}) \,|\, 0 < \widetilde{y} < 1\}$, $\{\widetilde{\mathbf{x}} = (\widetilde{x},0) \,|\, 0 < \widetilde{x} < 1\}$, and $\{\widetilde{\mathbf{x}} = (\widetilde{x},\widetilde{y}) \,|\, 0 < \widetilde{x} = \widetilde{y} < 1\}$, respectively. We write $\{\widetilde{y} \le \widetilde{x}\}$ for $\{\widetilde{\mathbf{x}} = (\widetilde{x},\widetilde{y}) \,|\, \widetilde{y} \le \widetilde{x}\}$. The origin will be denoted $\mathbf{0} = (0,0)$. The reference square and triangle are $\widehat{S} := (0,1)^2$ and $\widehat{T} := \{(\widehat{x},\widehat{y}) \,|\, 0 < \widehat{x} < 1, 0 < \widehat{y} < \widehat{x}\}$. The region covered by the reference patch will be denoted $\widetilde{S} := \widehat{S} = (0,1)^2$. It will be convenient to introduce $\widetilde{T} := \widehat{T}$ and set $\widetilde{T}^{\text{flip}} := \widetilde{S} \setminus \overline{\widetilde{T}}$. We denote the space of polynomials of total degree q by $\mathbb{P}_q = \text{span}\{x^i y^j \,|\, 0 \le i+j \le q\}$; the tensor product space $\mathbb{Q}_q$ is $\mathbb{Q}_q = \text{span}\{x^i y^j \,|\, 0 \le i,j \le q\}$.

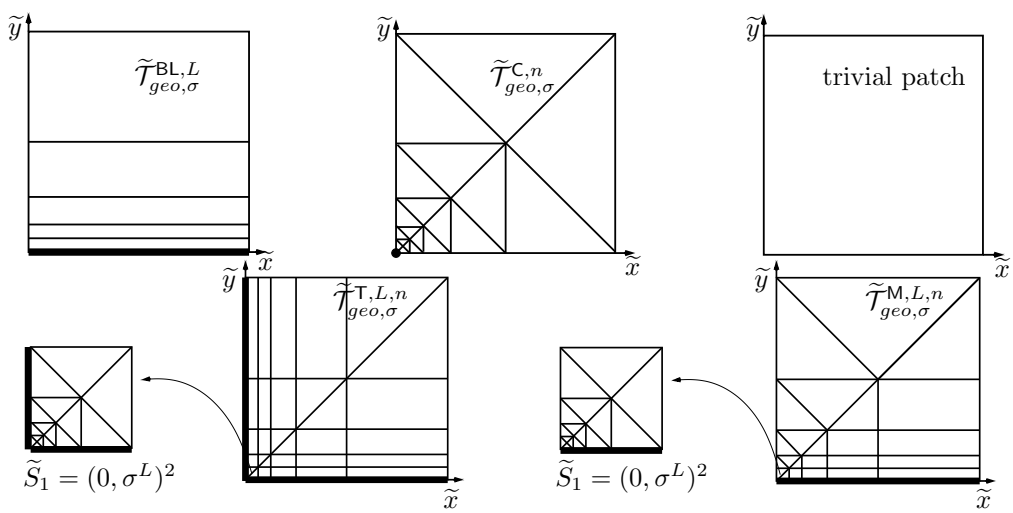

FIG. 2.1. *Patch mesh structures in axiparallel reference patch co-ordinates. Top row: reference boundary layer patch $\widetilde{\mathcal{T}}^{\mathsf{BL},L}_{geo,\sigma}$ with L layers of geometric refinement towards $\{\widetilde{y}=0\}$; reference corner patch $\widetilde{\mathcal{T}}^{\mathsf{C},n}_{geo,\sigma}$ with n layers of geometric refinement towards $(0,0)$; trivial patch. Bottom row: reference tensor patch $\widetilde{\mathcal{T}}^{\mathsf{T},L,n}_{geo,\sigma}$ with n layers of refinement towards $(0,0)$ and L layers of refinement towards $\{\widetilde{x}=0\}$ and $\{\widetilde{y}=0\}$; reference mixed patch $\widetilde{\mathcal{T}}^{\mathsf{M},L,n}_{geo,\sigma}$ with L layers of refinement towards $\{y=0\}$ and n layers of refinement towards $(0,0)$. Geometric entities shown in boldface indicate parts of $\partial\widetilde{S}$ that are mapped to $\partial\Omega$. These patch meshes are transported into the curvilinear polygon Ω shown in Fig. 1.1 via analytic patch maps $F_{K^{\mathcal{M}}}$.*

2. Macro triangulation. Geometric boundary layer mesh. Our robust exponentially convergent *hp* approximation is based on so-called geometric boundary layer meshes, denoted by $\mathcal{T}^{L,n}_{geo,\sigma}$. To facilitate our error analysis, the $\mathcal{T}^{L,n}_{geo,\sigma}$ are generated as push-forwards of a small number of so-called reference patches, which are partitions of $\widetilde{S}$, under the patch maps. The images of $\widetilde{S}$ under the patch maps form a (coarse) macro triangulation of Ω satisfying some minimal conditions, which are described in Section 2.1. This concept was also used in the context of *hp*-FEM for singular perturbations in [18, Sec. 3.3.3] and in [11].

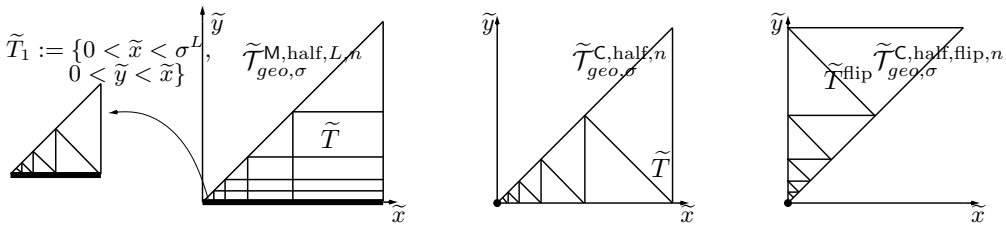

Fig. 2.2. *From left to right: half-patches* $\widetilde{\mathcal{T}}^{\mathsf{M},\mathrm{half},L,n}_{geo,\sigma}$, $\widetilde{\mathcal{T}}^{\mathsf{C},\mathrm{half},n}_{geo,\sigma}$, *and* $\widetilde{\mathcal{T}}^{\mathsf{C},\mathrm{half},\mathrm{flip},n}_{geo,\sigma}$. *They are given by the elements of* $\widetilde{\mathcal{T}}^{\mathsf{C},n}_{geo,\sigma}$ *and* $\widetilde{\mathcal{T}}^{\mathsf{M},L,n}_{geo,\sigma}$ *below the diagonal* $\{\widetilde{y} = \widetilde{x}\}$ *and the mirror image of* $\widetilde{\mathcal{T}}^{\mathsf{C},\mathrm{half},n}_{geo,\sigma}$ *at the diagonal* $\{\widetilde{y} = \widetilde{x}\}$.

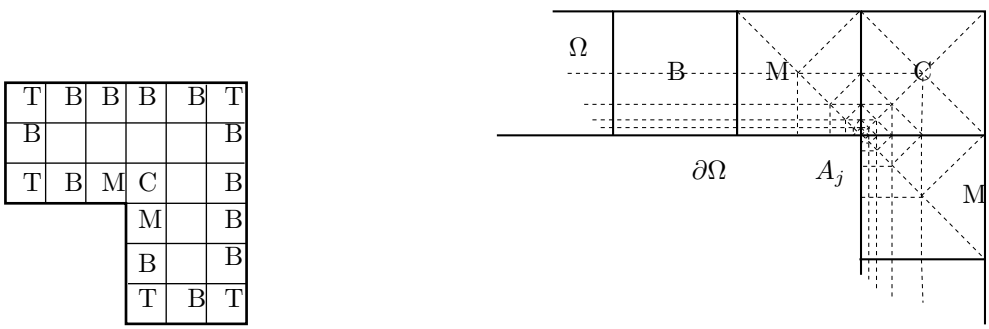

Fig. 2.3. *Left panel: example of an L-shaped domain decomposed into 27 patches (T, B, M, C indicate tensor, boundary layer, mixed, corner patches; empty squares stand for trivial patches). Right panel: Zoom-in near the reentrant corner.*

2.1. Macro triangulations. We assume given a fixed macro-triangulation $\mathcal{T}^{\mathcal{M}} = \{K^{\mathcal{M}} \,|\, K^{\mathcal{M}} \in \mathcal{T}^{\mathcal{M}}\}$ of Ω consisting of curvilinear quadrilaterals $K^{\mathcal{M}}$ with bijective element maps $F_{K^{\mathcal{M}}} : \widetilde{S} \to K^{\mathcal{M}}$ that are analytic in $\overline{\widetilde{S}}$ and that in addition satisfy the usual compatibility conditions. I.e., the partition $\mathcal{T}^{\mathcal{M}}$ does not have hanging nodes and, for any two distinct elements $K_1^{\mathcal{M}}, K_2^{\mathcal{M}} \in \mathcal{T}^{\mathcal{M}}$ that share an edge e, their respective element maps induce compatible parametrizations of e (cf., e.g., [18, Def. 2.4.1] for the precise conditions).

Each element of the fixed macro-triangulation $\mathcal{T}^{\mathcal{M}}$ is further subdivided according to one of the refinement patterns in Definition 2.1 (see also [18, Sec. 3.3.3] or [11]). The actual triangulation is then obtained by transplanting refinement patterns on the square reference patch $\widetilde{S}$ into the physical domain Ω by means of the element maps of the macro-triangulation, i.e., by the patch maps $F_{K^{\mathcal{M}}}$, resulting in the actual triangulation $\mathcal{T}$. Then, for any element $K \in \mathcal{T}$, the element maps $F_K : \widehat{K} \to K$ are concatenations of affine maps $A_K : \widehat{K} \to \widetilde{K}$, which realize the mapping from $\widehat{K} \in \{\widehat{S}, \widehat{T}\}$ to the elements in the patch refinement pattern, and the analytic patch maps $F_{K^{\mathcal{M}}}$. That is, the element maps have the form $F_K = F_{K^{\mathcal{M}}} \circ A_K$ for an affine A_K. Throughout the article, we will denote by $\widehat{K} \in \{\widehat{S}, \widehat{T}\}$ the reference element corresponding to an element K of a triangulation, and we will denote by $\widetilde{K}$ the elements of the triangulation of the reference patterns. Points in the reference patch $\widetilde{S}$ are denote $\widetilde{\mathbf{x}} = (\widetilde{x}, \widetilde{y}) \in \widetilde{S}$; variables (x, y) are employed to indicate points in Ω, and $\widehat{\mathbf{x}} = (\widehat{x}, \widehat{y})$ are used for point of the reference square $\widehat{S}$ and reference triangle $\widehat{T}$.

2.2. Refinement patterns in the reference configuration. The following refinement patterns, which are depicted in Fig. 2.1, are based on geometric refinement

towards a vertex and/or an edge; the parameter L controls the number of layers of refinement towards an edge whereas the natural number $n \geq L$ measures the number of geometric refinements towards vertices.

DEFINITION 2.1 (admissible refinement patterns). *Given $\sigma \in (0,1)$, L, $n \in \mathbb{N}_0$ with $n \geq L$ the following refinement patterns are admissible:*

1. *The trivial patch: The reference square $\widetilde{S}$ is not further refined. The corresponding triangulation of $\widetilde{S}$ consists of the single element: $\widehat{\mathcal{T}} = \{\widetilde{S}\}$.*
2. *The geometric boundary layer patch $\widetilde{\mathcal{T}}^{\mathsf{BL},L}_{geo,\sigma}$: $\widetilde{S}$ is refined anisotropically towards $\{\widetilde{y} = 0\}$ into L elements as depicted in Fig. 2.1 (top left). The mesh $\widetilde{\mathcal{T}}^{\mathsf{BL},L}_{geo,\sigma}$ is characterized by the nodes $(0,0)$, $(0,\sigma^i)$, $(1,\sigma^i)$, $i = 0,\ldots,L$, and the corresponding rectangular elements generated by these nodes.*
3. *The geometric corner patch $\widetilde{\mathcal{T}}^{\mathsf{C},n}_{geo,\sigma}$: $\widetilde{S}$ is refined isotropically towards $(0,0)$ as depicted in Fig. 2.1 (top middle). Specifically, the reference geometric corner patch mesh $\widetilde{\mathcal{T}}^{\mathsf{C},n}_{geo,\sigma}$ in $\widetilde{S}$ with geometric refinement towards $(0,0)$ and n layers is given by triangles and based on the nodes $(0,0)$, and $(0,\sigma^i)$, $(\sigma^i,0)$, (σ^i,σ^i), $i = 0,1,...,n$.*
4. *The tensor product patch $\widetilde{\mathcal{T}}^{\mathsf{T},L,n}_{geo,\sigma}$: $\widetilde{S}$ is triangulated in $\widetilde{S}_1 := (0,\sigma^L)^2$ and $\widetilde{S}_2 := \widetilde{S} \setminus \widetilde{S}_1$ separately as depicted in Fig. 2.1 (bottom left). The triangulation of $\widetilde{S}_1$ is a scaled version of $\widetilde{\mathcal{T}}^{\mathsf{C},n-L}_{geo,\sigma}$ and based on the nodes $(0,\sigma^i)$, $(\sigma^i,0)$, $i = L,\ldots,n$. The triangulation of $\widetilde{S}_2$ is based on the nodes (σ^i,σ^j), i, $j = 0,\ldots,L$.*
5. *The mixed patches $\widetilde{\mathcal{T}}^{\mathsf{M},L,n}_{geo,\sigma}$: The triangulation consists of both anisotropic elements and isotropic elements as depicted in Fig. 2.1 (bottom right) and is obtained by triangulating the regions $\widetilde{S}_1 := (0,\sigma^L)^2$, $\widetilde{S}_2 := \big(\widetilde{S} \setminus \widetilde{S}_1\big) \cap \{\widetilde{y} \leq \widetilde{x}\}$, $\widetilde{S}_3 := \widetilde{S} \setminus (\widetilde{S}_1 \cup \widetilde{S}_2)$ separately. The set $\widetilde{S}_1$ is a scaled version of $\widetilde{\mathcal{T}}^{\mathsf{C},n-L}_{geo,\sigma}$ based on the nodes $(0,\sigma^i)$, $(\sigma^i,0)$, $i = L,\ldots,n$. The triangulation of $\widetilde{S}_2$ is based on the nodes $(\sigma^i,0)$, (σ^i,σ^j), $0 \leq i \leq L$, $i \leq j \leq L$ and consists of rectangles and triangles, and only the triangles abut on the diagonal $\{\widetilde{x} = \widetilde{y}\}$. The triangulation of $\widetilde{S}_3$ consists of triangles only and is based on the nodes $(0,\sigma^i)$, (σ^i,σ^i), $i = 0,\ldots,L$.*

REMARK 2.2. *We kept the list of admissible patch refinement patterns in Definition 2.1 small in order to reduce the number of cases to be discussed for the hp-FE error bounds. A larger number of refinement patterns provides greater flexibility in the mesh generation. In particular, the reference patch meshes of Def. 2.1 do not contain general quadrilaterals but only rectangles; this restriction is not essential but leads to some simplifications in the hp-FE error analysis. Also certain types of anisotropic triangles (e.g., splitting anisotropic rectangles along the diagonal), which are altogether excluded in the present analysis, could be accommodated at the expense of additional technicalities.*

The addition of the diagonal line in the reference corner, tensor, and mixed patches is done to be able to apply the regularity theory of [18]. It is likely not necessary in actual computations. We also mention that with additional constraints on the macro triangulation $\mathcal{T}^{\mathcal{M}}$ the diagonal line could be dispensed with in certain situations as is illustrated in Section 2.4. ∎

2.3. Geometric boundary layer mesh. The following definition of the geometric boundary layer mesh $\mathcal{T}^{L,n}_{geo,\sigma}$ formalizes the patchwise construction of meshes on Ω based on transplanting the meshes of the reference configurations to Ω via the

patch maps $F_{K^{\mathcal{M}}}$.

Definition 2.3 (geometric boundary layer mesh $\mathcal{T}^{L,n}_{geo,\sigma}$ in Ω). *Let $\mathcal{T}^{\mathcal{M}}$ be a fixed macro-triangulation consisting of quadrilaterals with analytic element maps that satisfy [18, Def. 2.4.1].*

Given $\sigma \in (0,1)$, L, $n \in \mathbb{N}_0$ with $n \geq L$, a regular mesh $\mathcal{T}^{L,n}_{geo,\sigma}$ in Ω is called a geometric boundary layer mesh if the following conditions are satisfied:

1. *$\mathcal{T}^{L,n}_{geo,\sigma}$ is obtained by refining each element $K^{\mathcal{M}} \in \mathcal{T}^{\mathcal{M}}$ according to one of the refinement patterns given in Definition 2.1 using the given parameters σ, L, and n.*
2. *The resulting mesh $\mathcal{T}^{L,n}_{geo,\sigma}$ is a regular triangulation of Ω, i.e., it does not have hanging nodes. Since the element maps for the refinement patterns are assumed to be affine, this requirement ensures that the resulting triangulation satisfies [18, Def. 2.4.1].*

For each macro-element $K^{\mathcal{M}} \in \mathcal{T}^{\mathcal{M}}$, exactly one of the following cases is possible:

3. *$\overline{K^{\mathcal{M}}} \cap \partial\Omega = \emptyset$. Then the trivial patch is selected as reference patch.*
4. *$K^{\mathcal{M}}$ satisfies $\overline{K^{\mathcal{M}}} \cap \partial\Omega = \{\boldsymbol{A}_j\}$ for a vertex $\boldsymbol{A}_j$ of Ω. Then the corresponding reference patch is the corner patch $\widetilde{\mathcal{T}}^{\mathsf{C},n}_{geo,\sigma}$. Additionally, $F_{K^{\mathcal{M}}}(\mathbf{0}) = \boldsymbol{A}_j$.*
5. *$\overline{K^{\mathcal{M}}} \cap \partial\Omega = \overline{e}$ for an edge e of $K^{\mathcal{M}}$ and neither endpoint of e is a vertex of Ω. Then the refinement pattern is the boundary layer patch $\widetilde{\mathcal{T}}^{\mathsf{BL},L}_{geo,\sigma}$ and additionally $F_{K^{\mathcal{M}}}(\{\widetilde{y} = 0\}) \subset \partial\Omega$.*
6. *$\overline{K^{\mathcal{M}}} \cap \partial\Omega = \overline{e}$ for an edge e of $K^{\mathcal{M}}$ and exactly one endpoint of e is a vertex $\boldsymbol{A}_j$ of Ω. Then the refinement pattern is the mixed layer patch $\widetilde{\mathcal{T}}^{\mathsf{M},L,n}_{geo,\sigma}$ and additionally $F_{K^{\mathcal{M}}}(\{\widetilde{y} = 0\}) \subset \partial\Omega$ as well as $F_{K^{\mathcal{M}}}(\mathbf{0}) = \boldsymbol{A}_j$.*
7. *Exactly two edges of a macro-element $K^{\mathcal{M}}$ are situated on $\partial\Omega$. Then the refinement pattern is the tensor patch $\widetilde{\mathcal{T}}^{\mathsf{T},L,n}_{geo,\sigma}$. Additionally, it is assumed that $F_{K^{\mathcal{M}}}(\{\widetilde{y} = 0\}) \subset \partial\Omega$, $F_{K^{\mathcal{M}}}(\{\widetilde{x} = 0\}) \subset \partial\Omega$, and $F_{K^{\mathcal{M}}}(\mathbf{0}) = \boldsymbol{A}_j$ for a vertex $\boldsymbol{A}_j$ of Ω.*
8. *$\overline{K^{\mathcal{M}}} \cap \partial\Omega$ is a single point $\boldsymbol{P}$ that is not a vertex of Ω. Then the refinement pattern is the corner patch $\widetilde{\mathcal{T}}^{\mathsf{C},L}_{geo,\sigma}$ with L layers of geometric mesh refinement towards $\boldsymbol{P}$. Additionally, it is assumed that $F_{K^{\mathcal{M}}}(\mathbf{0}) = \boldsymbol{P} \in \partial\Omega$.*

Finally, the following technical condition ensures the existence of certain meshlines:

9. *For each vertex $\boldsymbol{A}_j$ of Ω, introduce a set of lines*

$$\ell = \bigcup_{K^{\mathcal{M}}:\, \boldsymbol{A}_j \in \overline{K^{\mathcal{M}}}} \{\, F_{K^{\mathcal{M}}}(\{\widetilde{y} = 0\}), F_{K^{\mathcal{M}}}(\{\widetilde{x} = 0\}), F_{K^{\mathcal{M}}}(\{\widetilde{x} = \widetilde{y}\})\,\}.$$

Let Γ_j, Γ_{j+1} be the two boundary arcs of Ω that meet at $\boldsymbol{A}_j$. Then there exists a line $e \in \ell$ such that the interior angles $\angle(e, \Gamma_j)$ and $\angle(e, \Gamma_{j+1})$ are both less than π.

Remark 2.4. *The last condition, requirement 9. in Definition 2.3, is merely a technical condition that results from our applying the regularity theory for singular perturbations of [18]. Very likely, it could be dropped.*

The condition that $F_{K^{\mathcal{M}}}(\mathbf{0}) \in \partial\Omega$ or that $F_{K^{\mathcal{M}}}(\{\widetilde{y} = 0\}) \subset \partial\Omega$ are not conditions on the patch geometry but on the maps $F_{K^{\mathcal{M}}}$. They are not essential but introduced for notational simplicity. They could be enforced by suitably concatenating the maps $F_{\mathcal{K}^{\mathcal{M}}}$ with an orthogonal transformation. ∎

Remark 2.5. *The meshes $\mathcal{T}^{L,n}_{geo,\sigma}$ are refined towards both vertices and edges of Ω. The parameter $L \in \mathbb{N}_0$ measures the number of layers of geometric refinement towards $\partial\Omega$ whereas the parameter $n \in \mathbb{N}$ characterizes the number of layers of geometric*

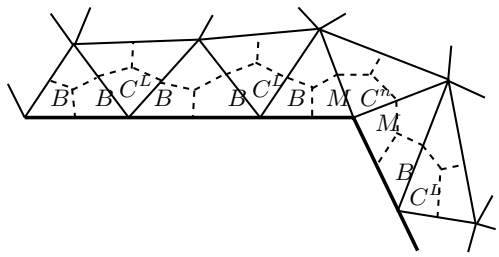

FIG. 2.4. *Generating a boundary layer mesh from a regular triangulation $\mathcal{T}^0$: solid lines are the triangulation $\mathcal{T}^0$, dashed lines connect edge midpoints with element barycenters to create a mesh consisting of quadrilaterals. B stands for boundary layer, M for mixed, C^L for corner layer patches $\widetilde{\mathcal{T}}^{\mathsf{C},L}_{geo,\sigma}$, C^n for corner layer patches $\widetilde{\mathcal{T}}^{\mathsf{C},n}_{geo,\sigma}$, empty quadrilaterals are trivial patches.*

refinement towards the vertices. For $L = 0$ (or, more generally, L fixed), the meshes $\mathcal{T}^{0,n}_{geo,\sigma}$, $n = 1, 2, \ldots$, realize the "geometric meshes" introduced in [3, 4] (see also [29, Sec. 4.4.1]) for the hp-FEM applied to elliptic boundary value problems with piecewise analytic data. ∎

EXAMPLE 2.6. *Fig. 2.3 (left and middle) shows an example of an L-shaped domain with macro triangulation and suitable refinement patterns.* ∎

2.4. Geometric boundary layer meshes in curvilinear polygons. Geometric boundary layer meshes can be constructed in various ways. A first approach, which is in line with the illustration in Fig. 2.3, is to create one layer of quadrilateral elements that partition a tubular neighborhood $T_{\partial\Omega}$ of $\partial\Omega$. Each quadrilateral K should fall into one of the following 3 categories: a) $\overline{K} \cap \partial\Omega$ is an edge of K; b) $\overline{K} \cap \partial\Omega$ consists of two contiguous edges and the shared vertex is a vertex of Ω; c) $\overline{K} \cap \partial\Omega$ is a vertex of Ω. In the second step, refinement patterns from Definition 2.3 are applied to each quadrilateral. In the final step, $\Omega' := \Omega \backslash T_{\partial\Omega}$ is triangulated under the constraint that the boundary nodes of the triangulation of Ω' on $\partial\Omega'$ coincide with the nodes of the triangulation of $T_{\partial\Omega}$ that also lie on $\partial\Omega'$. This triangulation of Ω' could be chosen to consist of triangles (and/or quadrilaterals). All elements of that triangulation will be denoted "trivial patches"; we mention without proof that the approximation result holds also if we include "trivial" triangles in the list of refinement patterns.

Geometric boundary layer meshes can also be constructed for general (curvilinear) polygons Ω starting from any regular initial triangulation $\mathcal{T}^0$ of Ω. This triangulation $\mathcal{T}^0$ is assumed to consist of (curvilinear) triangles with analytic element maps and satisfying the "usual" conditions for triangulations as spelled out in [18, Def. 2.4.1]. Then, the geometric boundary layer mesh is generated in 3 steps (cf. Fig. 2.4):

1. (Ensure condition 9 of Def. 2.3) For each vertex $\boldsymbol{A}_j$ of Ω verify if an edge e of $\mathcal{T}^0$ splits the interior angle at $\boldsymbol{A}_j$ into two angles each less than π. If not, then suitably split an appropriate triangle abuting on $\boldsymbol{A}_j$ into two triangles (so that the newly introduced edge will satisfy this condition) and remove the newly introduced hanging node by a mesh closure. The resulting triangulation has again analytic element maps and satisfies [18, Def. 2.4.1]; it is again denoted $\mathcal{T}^0$.
2. (Create a macro triangulation $\mathcal{T}^{\mathcal{M}}$ consisting of quadrilaterals only.) Split each triangle $K \in \mathcal{T}^0$ into 3 quadrilaterals as follows: split the reference triangle $\widehat{T}$ into 3 quadrilaterals $\widehat{K}_i$, $i = 1, 2, 3$, characterized by the vertices of $\widehat{T}$, its barycenter, and by the 3 midpoints of the edges of $\widehat{T}$. The element

maps of the 3 quadrilaterals $F_K(\widehat{K}_i)$, $i = 1, 2, 3$, are obtained by concatenating the bilinear bijections $F_{\widehat{K}_i} : \widetilde{S} \to \widehat{K}_i$ with F_K. The triangulation $\mathcal{T}^{\mathcal{M}}$ of Ω obtained in this way realizes a decomposition of Ω into (curvilinear) quadrilaterals, and the element maps satisfy [18, Def. 2.4.1].

3. (Generate the geometric boundary layer mesh.) The refinement pattern for each $K \in \mathcal{T}^{\mathcal{M}}$ is determined since K falls into exactly one of the categories 3—8 of Definition 2.3 as can be seen by the following observations: a) At most 2 edges of K are on $\partial\Omega$ (since the two edges that meet in the barycenter of the parent triangle cannot be on $\partial\Omega$). b) If two edges of K are situated on $\partial\Omega$, then they have to be subsets of the two edges of the parent triangle with common vertex $\boldsymbol{V}$; since $\mathcal{T}^0$ is a regular triangulation, the common vertex $\boldsymbol{V}$ has to be a vertex of Ω. Additionally, if necessary, the assumptions on where the reference element vertex $\mathbf{0}$ and/or the edges $\{\widetilde{y} = 0\}$, $\{\widetilde{x} = 0\}$ are mapped can be ensured by suitably adjusting the element map with the aid of an orthogonal transformation of $\widetilde{S}$. Finally, condition 9 of Def. 2.3 is satisfied by step 1.

It remains to see that after selecting the refinement patterns the resulting triangulation satisfies [18, Def. 2.4.1]. This follows from the fact that the parameters σ, L, n are the same for all macro elements and the structure of the refinement patterns: If an edge e of the macro triangulation inherits a further refinement from a refinement pattern, then the edge either lies on $\partial\Omega$ (which is immaterial for the question of satisfying [18, Def. 2.4.1]) or it is in Ω and exactly one of its endpoints $\boldsymbol{V}$ lies on $\partial\Omega$. This edge e is shared by two macro elements. If $\boldsymbol{V}$ is a vertex of Ω, then the refinement patterns are such that the induced 1D-mesh on e is the same geometric mesh with n layers for both macro elements. If $\boldsymbol{V} \in \partial\Omega$ is not a vertex of Ω, then the induced 1D-mesh on e is the same geometric mesh with L layers for both macro elements. Hence, the resulting mesh satisfies [18, Def. 2.4.1].

2.5. Properties of the mesh patches. We note that parts of the mixed patch, the tensor patch, and the corner patch are identical or at least structurally similar. For the analysis of the approximation properties of *hp*-FEM on geometric boundary layer meshes it is therefore convenient to single out these meshes:

Definition 2.7 (half-patches, cf. Fig. 2.2). *The* <u>*mixed half-patch*</u> $\widetilde{\mathcal{T}}^{\mathsf{M},\mathrm{half},L,n}_{geo,\sigma}$ *and the* <u>*corner half-patch*</u> $\widetilde{\mathcal{T}}^{\mathsf{C},\mathrm{half},n}_{geo,\sigma}$ *on* $\widetilde{T} = \{(\widetilde{x}, \widetilde{y}) \,|\, 0 < \widetilde{x} < 1, 0 < \widetilde{y} < \widetilde{x}\}$ *are obtained by restricting* $\widetilde{\mathcal{T}}^{\mathsf{M},L,n}_{geo,\sigma}$ *and* $\widetilde{\mathcal{T}}^{\mathsf{C},n}_{geo,\sigma}$ *to* $\widetilde{T}$. *The* <u>*flipped corner half-patch*</u> $\widetilde{\mathcal{T}}^{\mathsf{C},\mathrm{half},\mathrm{flip},n}_{geo,\sigma}$ *on* $\widetilde{T}^{\mathrm{flip}} := \{(\widetilde{x}, \widetilde{y}) \,|\, 0 < \widetilde{x} < 1, \widetilde{x} < \widetilde{y} < 1\}$ *is obtained by reflecting* $\widetilde{\mathcal{T}}^{\mathsf{C},\mathrm{half},n}_{geo,\sigma}$ *at the diagonal* $\{(\widetilde{x}, \widetilde{x}) \,|\, \widetilde{x} \in (0, 1)\}$ *of* $\widetilde{S}$.

We will approximate functions on boundary layer meshes $\mathcal{T}^{L,n}_{geo,\sigma}$ with the aid of an elementwise defined operator Π_q. To estimate the total error in L^2-based norms, the elemental error contributions are summed up on each mesh patch separately. The following Lemma 2.8 provides tools to conveniently do that. In order to formulate Lemma 2.8, we introduce some additional notation, which represents the pull-back of the parts of the boundary of the reference patch that is mapped to $\partial\Omega$ and is marked by bold lines or dots in Figs. 2.1 and 2.2:

$$\Gamma^C := \Gamma^{\mathsf{C},\mathrm{half}} := \Gamma^{\mathsf{C},\mathrm{half},\mathrm{flip}} := \{\mathbf{0}\}, \tag{2.1a}$$

$$\Gamma^{\mathsf{BL}} := \Gamma^M := \Gamma^{\mathsf{M},\mathrm{half}} := \{\widetilde{y} = 0\}, \tag{2.1b}$$

$$\Gamma^{\mathsf{T}} := \{\widetilde{y} = 0\} \cup \{\widetilde{x} = 0\} \cup \{\mathbf{0}\}. \tag{2.1c}$$

LEMMA 2.8 (properties of mesh patches). *The reference patches (cf. Def. 2.1) and half patches (cf. Def. 2.7) have the following properties:*

(i) The triangular elements $\widetilde{K}$ of the reference patches are shape regular with shape regularity constant depending solely on σ. For the rectangular elements $\widetilde{K}$ of the reference patches, the element maps $A_{\widetilde{K}} : \widehat{K} \to \widetilde{K}$ are affine with

$$A'_{\widetilde{K}} = \begin{pmatrix} h_{\widetilde{K},\widetilde{x}} & \\ & h_{\widetilde{K},\widetilde{y}} \end{pmatrix},$$

where $h_{\widetilde{K},\widetilde{x}}$, $h_{\widetilde{K},\widetilde{y}} \leq 1$ are the side lengths (in $\widetilde{y}$ and $\widetilde{x}$-direction) of $\widetilde{K}$. We denote

$$h_{\widetilde{K},min} := \min\{h_{\widetilde{K},\widetilde{x}}, h_{\widetilde{K},\widetilde{y}}\}, \qquad h_{\widetilde{K},max} := \max\{h_{\widetilde{K},\widetilde{x}}, h_{\widetilde{K},\widetilde{y}}\}. \tag{2.2}$$

(ii) There is $c_{\text{dist}} > 0$ depending only on σ such that for all triangular elements $\widetilde{K}$ of a reference patch $\widetilde{\mathcal{T}}$ or a half-patch $\widetilde{\mathcal{T}}$ the following dichotomy holds:

$$\text{either } \overline{\widetilde{K}} \cap \Gamma \neq \emptyset \quad \text{or} \quad \operatorname{dist}(\widetilde{K}, \Gamma) \geq c_{\text{dist}} h_{\widetilde{K}},$$

where $h_{\widetilde{K}} = \operatorname{diam}(\widetilde{K})$ and $\Gamma \in \{\Gamma^{\mathsf{C}}, \Gamma^{\mathsf{C,half}}, \Gamma^{\mathsf{C,half,flip}}, \Gamma^{\mathsf{T}}, \Gamma^{\mathsf{M}}, \Gamma^{\mathsf{M,half}}, \Gamma^{\mathsf{BL}}\}$ for $\widetilde{\mathcal{T}} \in \{\widetilde{\mathcal{T}}^{\mathsf{C},n}_{geo,\sigma}, \widetilde{\mathcal{T}}^{\mathsf{C,half},n}_{geo,\sigma}, \widetilde{\mathcal{T}}^{\mathsf{C,half,flip},n}_{geo,\sigma}, \widetilde{\mathcal{T}}^{\mathsf{T},n}_{geo,\sigma}, \widetilde{\mathcal{T}}^{\mathsf{M},L,n}_{geo,\sigma}, \widetilde{\mathcal{T}}^{\mathsf{M,half},L,n}_{geo,\sigma}, \widetilde{\mathcal{T}}^{\mathsf{BL},L}_{geo,\sigma}\}$, respectively.

(iii) There is $c_{\text{dist}} > 0$ depending only on σ such that for all rectangular elements $\widetilde{K}$ of a reference patch $\widetilde{\mathcal{T}}$ or half-patch $\widetilde{\mathcal{T}}$, the following dichotomy holds:

$$\text{Either } \overline{\widetilde{K}} \cap \Gamma = \emptyset \quad \text{or} \quad \operatorname{dist}(\widetilde{K}, \Gamma) \geq c_{\text{dist}} h_{\widetilde{K},min},$$

where $\Gamma \in \{\Gamma^{\mathsf{T}}, \Gamma^{\mathsf{M}}, \Gamma^{\mathsf{M,half}}, \Gamma^{\mathsf{BL}}\}$ for $\widetilde{\mathcal{T}} \in \{\widetilde{\mathcal{T}}^{\mathsf{T},n}_{geo,\sigma}, \widetilde{\mathcal{T}}^{\mathsf{M},L,n}_{geo,\sigma}, \widetilde{\mathcal{T}}^{\mathsf{M,half},L,n}_{geo,\sigma}, \widetilde{\mathcal{T}}^{\mathsf{BL},L}_{geo,\sigma}\}$, respectively.

(iv) There is $c_{\text{dist}} > 0$ depending only on σ such that for all rectangular elements $\widetilde{K}$ of a mixed patch, a mixed half-patch, or a tensor patch there holds $\operatorname{dist}(\widetilde{K}, \mathbf{0}) \geq c_{\text{dist}} h_{\widetilde{K},max}$.

(v) There is $C > 0$ depending only on σ such that for all elements $\widetilde{K}$ of a reference patch or half-patch there holds $\operatorname{dist}(\widetilde{K}, \mathbf{0}) \leq C \operatorname{diam} \widetilde{K}$.

(vi) Let $\delta > 0$ and consider a reference patch or half-patch. Let $\widetilde{\mathcal{T}}^{\triangle}$ be the collection of triangles of that reference patch or half-patch that do not abut on the vertex $\mathbf{0}$. Then, there exists a constant $C > 0$ depending solely on δ and σ such that

$$\sum_{\widetilde{K} \in \widetilde{\mathcal{T}}^{\triangle}} h^{\delta}_{\widetilde{K}} \leq C.$$

(vii) Let $\delta > 0$ and consider a reference mixed patch, tensor patch, mixed half-patch or corner half-patch. Let $\widetilde{\mathcal{T}}^{\square}$ be the collection of rectangles of that reference patch. Then there exists a constant $C > 0$ depending solely on δ and the parameter σ such that

$$\sum_{\widetilde{K} \in \widetilde{\mathcal{T}}^{\square}} \frac{h_{\widetilde{K},min}}{h_{\widetilde{K},max}} h^{\delta}_{\widetilde{K},max} \leq C.$$

(viii) *Let $\delta \in (0,1]$, $\alpha > 0$, and consider a reference patch or half-patch. Let $\widetilde{\mathcal{T}}^{\triangle}$ be the collection of triangles of that reference patch or half-patch that do not abut on the vertex $\mathbf{0}$. Then, there holds, with a $C > 0$ depending solely on δ, α, and σ,*

$$\forall \varepsilon \in (0,1]: \qquad \sum_{\widetilde{K} \in \widetilde{\mathcal{T}}^{\triangle}} (h_{\widetilde{K}}/\varepsilon)^{\delta} e^{-\alpha h_{\widetilde{K}}/\varepsilon} \le C.$$

(ix) *Let $\delta \in (0,1]$, $\alpha > 0$, and consider a reference mixed patch, mixed half-patch, or a reference tensor patch. Let $\widetilde{\mathcal{T}}^{\square}$ be the collection of rectangles of that reference patch. Then there exists a constant $C > 0$ depending solely on δ, α, and σ such that*

$$\forall \varepsilon \in (0,1]: \qquad \sum_{\widetilde{K} \in \widetilde{\mathcal{T}}^{\square}} \frac{h_{\widetilde{K},min}}{h_{\widetilde{K},max}} (h_{\widetilde{K},max}/\varepsilon)^{\delta} e^{-\alpha h_{\widetilde{K},max}/\varepsilon} \le C.$$

Proof. Items (i)–(v) follow by construction.

Since items (vi), (vii) are shown by similar arguments, we only prove the case of (vii) for the specific case of the mixed patch as shown in Fig. 2.1, bottom right panel. Inspection of that panel shows that for each $\widetilde{K} \in \widetilde{\mathcal{T}}^{\square}$ we have $h_{\widetilde{K},min} = h_{\widetilde{K},\widetilde{y}}$ and $h_{\widetilde{K},max} = h_{\widetilde{K},\widetilde{x}}$. Additionally, the elements can be enumerated as $K_{i,j}$, $i = 1, \dots, L$, $j = 1, \dots, i$ with $h_{K_{i,j},x} \sim \sigma^{L-i}$, $h_{K_{i,j},y} \sim \sigma^{L-j}$. Hence,

$$\sum_{\widetilde{K} \in \widetilde{\mathcal{T}}^{\square}} \frac{h_{\widetilde{K},min}}{h_{\widetilde{K},max}} h_{\widetilde{K},max}^{\delta} \lesssim \sum_{i=1}^{L} \sum_{j=1}^{i} \frac{\sigma^{L-j}}{\sigma^{L-i}} \sigma^{(L-i)\delta} \lesssim \sum_{i=1}^{L} \sigma^{\delta(L-i)} \lesssim 1. \tag{2.3}$$

The proof of items (viii), (ix) is also done in similar ways. Therefore, we will only show (ix). The key observation is that by comparing sums with integrals, there is a constant $C > 0$ depending solely on δ, α, and σ such that

$$\forall \varepsilon \in (0,1]: \qquad \sum_{i=0}^{\infty} (\sigma^i/\varepsilon)^{\delta} e^{-\alpha \sigma^i/\varepsilon} \le C. \tag{2.4}$$

The proof of (ix) now follows by a reasoning similar to that in (2.3). ∎

3. Approximation on the reference elements and on the reference configurations. In Sec. 3.1 we construct polynomial approximation operators on the reference square and triangle that coincide with the Gauss-Lobatto interpolant on the edges, which affords convenient H^1-conforming approximations. Sec. 3.2 studies the approximation properties of spaces of piecewise polynomials on the reference patches. It is shown that functions of boundary layer or corner layer type can be approximated at exponential rates, robustly in the parameter ε that characterizes the strength of the layer.

3.1. Polynomial approximation operators on the reference element. We introduce polynomial approximation operators on the reference triangle $\widehat{T}$ in Lemma 3.1 and the reference square $\widehat{S}$ in Lemma 3.2. Before actually doing so, we highlight a technical detail: the triangular elements (on the reference patches) are shape-regular so that isotropic scaling arguments can be brought to bear; only the rectangles (of the reference patches) may be anisotropic, for which tensor product polynomial approximation operators (specifically, the Gauss-Lobatto interpolation operator) are used for their favorable anisotropic scaling properties.

LEMMA 3.1 (element-by-element approximation on triangles). *Let $\widehat{T}$ be the reference triangle. Then for every $q \in \mathbb{N}$, there exists a linear operator $\widehat{\Pi}_q^{\triangle} : C(\overline{\widehat{T}}) \to \mathbb{P}_q$ with the following properties:*

(i) For each edge e of $\widehat{T}$, $(\widehat{\Pi}_q^{\triangle} u)|_e$ coincides with the Gauss-Lobatto interpolant i_q of $u|_e$ on edge e.

(ii) (projection property) $\widehat{\Pi}_q^{\triangle} v = v$ for all $v \in \mathbb{P}_q$.

(iii) (stability) There exists a constant $C > 0$ such that for every $q \in \mathbb{N}$ there holds

$$\forall u \in W^{1,\infty}(\widehat{T}): \qquad \|u - \widehat{\Pi}_q^{\triangle} u\|_{W^{1,\infty}(\widehat{T})} \le C q^4 \|\nabla u\|_{L^\infty(\widehat{T})},$$
$$\forall u \in C(\overline{\widehat{T}}): \qquad \|u - \widehat{\Pi}_q^{\triangle} u\|_{L^\infty(\widehat{T})} \le C q^2 \|u\|_{L^\infty(\widehat{T})}.$$

(iv) Let $\boldsymbol{A}$ be one of the vertices of $\widehat{T}$ and $\beta \in [0,1)$. Then there is $C > 0$ (depending only on β) such that, provided the right-hand side is finite,

$$\|u - \widehat{\Pi}_q^{\triangle} u\|_{L^\infty(\widehat{T})} + \|u - \widehat{\Pi}_q^{\triangle} u\|_{H^1(\widehat{T})} \le C q^4 \| \operatorname{dist}(\cdot, \boldsymbol{A})^\beta \nabla^2 u\|_{L^2(\widehat{T})}.$$

(v) Let $u \in C^\infty(\widehat{T})$ satisfy, for some C_u, $\gamma > 0$ and for some h, $\varepsilon \in (0,1]$,

$$\forall n \in \mathbb{N}_0: \quad \|\nabla^n u\|_{L^\infty(\widehat{T})} \le C_u \gamma^n h^n \max\{n+1, \varepsilon^{-1}\}^n.$$

Then there are δ, C, η, $b > 0$ depending solely on γ such that, under the provision that the <u>scale resolution condition</u>

$$\frac{h}{q\varepsilon} \le \delta \tag{3.1}$$

is satisfied, there holds

$$\begin{aligned}\|u - \widehat{\Pi}_q^{\triangle} u\|_{W^{1,\infty}(\widehat{T})} &\le C C_u \left(\left(\frac{h}{h+\eta}\right)^{q+1} + \left(\frac{h}{q\varepsilon\eta}\right)^{q+1} \right) \\ &\le C C_u e^{-bq} \min\{1, h/\varepsilon\}.\end{aligned}$$

Proof. The operator $\widehat{\Pi}_q^{\triangle}$ is taken as the one defined in [18, Thm. 3.2.20], where items (i)–(iii) are shown (the $W^{1,\infty}$-estimate follows with an additional polynomial inverse estimate). Item (iv) is taken from [18, Prop. 3.2.21]. For Item (v), we note that the projection property of (ii) and the stability assertions (iii) reduce the error estimate to a best approximation problem, which can be taken from [14, Lemma C.2].□

LEMMA 3.2 (approximation properties of the Gauss-Lobatto interpolant). *Let $\widehat{S}$ be the reference square. For each $q \in \mathbb{N}$ the tensor-product Gauss-Lobatto interpolation operator $\widehat{\Pi}_q^{\square} : C(\overline{\widehat{S}}) \to \mathbb{Q}_q$ satisfies the following:*

(i) (projection property) $\widehat{\Pi}_q^{\square} v = v$ for all $v \in \mathbb{Q}_q$.

(ii) For each edge e, the restriction $(\widehat{\Pi}_q^{\square} u)|_e$ coincides with the univariate Gauss-Lobatto interpolant i_q of $u|_e$ on e.

(iii) (stability)

$$\forall u \in C(\overline{\widehat{S}}): \qquad \|u - \widehat{\Pi}_q^{\square} u\|_{L^\infty(\widehat{S})} \le C q \|u\|_{L^\infty(\widehat{S})},$$
$$\forall u \in C^1(\overline{\widehat{S}}): \qquad \|\partial_{\widehat{x}}(u - \widehat{\Pi}_q^{\square} u)\|_{L^\infty(\widehat{S})} \le C q^4 \|\partial_x u\|_{L^\infty(\widehat{S})},$$
$$\forall u \in C^1(\overline{\widehat{S}}): \qquad \|\partial_{\widehat{y}}(u - \widehat{\Pi}_q^{\square} u)\|_{L^\infty(\widehat{S})} \le C q^4 \|\partial_y u\|_{L^\infty(\widehat{S})}.$$

(iv) Let $u \in C^\infty(\widehat{S})$ satisfy for some C_u, $\gamma > 0$, ε_x, ε_y, h_x, $h_y \in (0,1]$ and all $(n,m) \in \mathbb{N}_0^2$

$$\|\partial_{\widehat{x}}^m \partial_{\widehat{y}}^n u\|_{L^\infty(\widehat{S})} \le C_u \gamma^{n+m} h_x^m h_y^n \max\{n+1, \varepsilon_y^{-1}\}^n \max\{m+1, \varepsilon_x^{-1}\}^m. \tag{3.2}$$

Then there are constants δ, C, η, $b > 0$ depending solely on γ such that under the scale-resolution condition

$$\frac{h_x}{q\varepsilon_x} + \frac{h_y}{q\varepsilon_y} \le \delta \tag{3.3}$$

there holds

$$\begin{aligned}
&\|\partial_{\widehat{x}}(u - \widehat{\Pi}_q^\square u)\|_{L^\infty(\widehat{S})} \\
&\le C C_u \frac{h_x}{\varepsilon_x}\left[\varepsilon_x \left(\frac{h_x}{h_x+\eta}\right)^q + \left(\frac{h_x}{\varepsilon_x q\eta}\right)^q + \left(\frac{h_y}{h_y+\eta}\right)^{q+1} + \left(\frac{h_y}{\varepsilon_y q\eta}\right)^{q+1}\right], \\
&\|\partial_{\widehat{y}}(u - \widehat{\Pi}_q^\square u)\|_{L^\infty(\widehat{S})} \\
&\le C C_u \frac{h_y}{\varepsilon_y}\left[\left(\frac{h_x}{h_x+\eta}\right)^{q+1} + \left(\frac{h_x}{\varepsilon_x q\eta}\right)^{q+1} + \varepsilon_y \left(\frac{h_y}{h_y+\eta}\right)^q + \left(\frac{h_y}{\varepsilon_y q\eta}\right)^q\right], \\
&\|u - \widehat{\Pi}_q^\square u\|_{L^\infty(\widehat{S})} \\
&\le C C_u \left[\left(\frac{h_x}{h_x+\eta}\right)^{q+1} + \left(\frac{h_x}{\varepsilon_x q\eta}\right)^{q+1} + \left(\frac{h_y}{h_y+\eta}\right)^{q+1} + \left(\frac{h_y}{\varepsilon_y q\eta}\right)^{q+1}\right].
\end{aligned}$$

Proof. Items (i), (ii) are well-known. We let Λ_q denote the Lebesgue constant of the univariate Gauss-Lobatto interpolation operator of polynomial degree $q \in \mathbb{N}$ (cf. Lemma B.2). The L^∞-stability in (iii) follows from tensor product arguments, viz. $\|\widehat{\Pi}_q^\square u\|_{L^\infty(\widehat{S})} \le \Lambda_q^2 \|u\|_{L^\infty(\widehat{S})}$ and the (generous) bound $\Lambda_q^2 \le Cq$ for $q \ge 1$. For the remaining estimates, we introduce the tensor-product Gauss-Lobatto interpolation operator $\widehat{\Pi}_q^\square = i_q \otimes i_q = i_q^{\widehat{x}} \otimes i_q^{\widehat{y}}$, where we use the superscipts $\widehat{x}$ and $\widehat{y}$ to emphasize the variable with respect to which the univariate Gauss-Lobatto interpolant acts. From

$$u - i_q^{\widehat{y}} \otimes i_q^{\widehat{x}} u = u - (\mathrm{I} \otimes i_q^{\widehat{y}})u + \mathrm{I} \otimes i_q^{\widehat{y}}(u - i_q^{\widehat{x}} \otimes \mathrm{I}\, u)$$

we get in view of the univariate stability bound Lemma B.2

$$\begin{aligned}
\|\partial_{\widehat{x}}(u - i_q^{\widehat{x}} \otimes i_p^{\widehat{y}} u)\|_{L^\infty(\widehat{S})} &\lesssim \Lambda_q \sup_{\widehat{x}\in(0,1)} \inf_{v \in \mathbb{P}_q} \|\partial_{\widehat{x}} u(x,\cdot) - v\|_{L^\infty(0,1)} \\
&\quad + q^2 \Lambda_q^2 \sup_{\widehat{y}\in(0,1)} \inf_{v \in \mathbb{P}_q} \|\partial_{\widehat{x}}(u(\cdot,\widehat{y}) - v)\|_{L^\infty(0,1)};
\end{aligned} \tag{3.4}$$

an analogous estimate holds for $\partial_y(u - i_q^{\widehat{x}} \otimes i_q^{\widehat{y}} u)$. The estimate (3.4) gives the stability estimates in $W^{1,\infty}$ of (iii) by selecting $v = 0$ in the infima. The estimate (3.4) reduces the question of approximation on $\widehat{S}$ to questions of univariate polynomial approximation. The pertinent approximation results to prove item (iv) are given in Lemma B.1. ∎

3.2. Approximation on the reference patches. In this section, we study the approximation of functions on the reference patches (or the half-patches) described in Defs. 2.1, 2.7. The non-trivial reference patches consist of meshes that are refined towards $\mathbf{0}$, which can resolve algebraic singularities at $\mathbf{0}$, and meshes that are anisotropically refined towards the edge $\{\widetilde{y}=0\}$, which can resolve algebraic singularities at $\{\widetilde{y}=0\}$ or boundary layers. We show exponential approximability of functions that have algebraic singularities at $\mathbf{0}$ or boundary layers at $\{\widetilde{y}=0\}$.

Throughout this section, we will use the notation

$$\widetilde{r}(\cdot) := \operatorname{dist}(\mathbf{0},\cdot) \tag{3.5}$$

In this section, we present piecewise polynomial approximations on reference patches using the following elementwise defined interpolation operator:

$$(\widetilde{\Pi}_q)|_{\widetilde{K}} u := \begin{cases} \widehat{\Pi}_q^{\triangle}(u\circ A_{\widetilde{K}}) & \text{if } \widetilde{K} \text{ is a triangle } \triangle \\ \widehat{\Pi}_q^{\square}(u\circ A_{\widetilde{K}}) & \text{if } \widetilde{K} \text{ is a rectangle } \square, \end{cases} \tag{3.6}$$

where $A_{\widetilde{K}} : \widehat{K} \to \widetilde{K} = A_{\widetilde{K}}(\widehat{K}) \subset \widetilde{S}$ is the affine bijection between the reference element and the corresponding element on the reference patch. The edge-traces of the interpolators $\widehat{\Pi}_q^{\triangle}$ and $\widehat{\Pi}_q^{\square}$ coincide with the univariate Gauss-Lobatto interpolation operator on the edges of $\widehat{K}$. Hence, H^1-conformity of the elementwise defined operator $\widetilde{\Pi}_q$ is ensured. We will frequently use the stability estimates

$$\|\widetilde{\Pi}_q u\|_{L^\infty(\widetilde{K})} \le Cq^2\|u\|_{L^\infty(\widetilde{K})}, \qquad \|\nabla\widetilde{\Pi}_q u\|_{L^\infty(\widetilde{K})} \le Cq^4\|\nabla u\|_{L^\infty(\widetilde{K})}; \tag{3.7}$$

these estimates are easily seen to hold for triangles with the isotropic scaling property and Lemma 3.1, (iii). The anisotropic nature of the rectangles is accounted for by separately scaling the bounds for the partial derivatives in Lemma 3.2, (iii).

3.2.1. *hp*-FE approximation of corner singularity functions.

Lemma 3.3 (approximation of corner singularity functions).

(i) Let $\widetilde{\mathcal{T}} \in \{\widetilde{\mathcal{T}}^{\mathsf{M},\mathrm{half},L,n}_{geo,\sigma}, \widetilde{\mathcal{T}}^{\mathsf{C},\mathrm{half},n}_{geo,\sigma}, \widetilde{\mathcal{T}}^{\mathsf{C},\mathrm{half,flip},n}_{geo,\sigma}, \widetilde{\mathcal{T}}^{\mathsf{C},n}_{geo,\sigma}, \widetilde{\mathcal{T}}^{\mathsf{T},n}_{geo,\sigma}\}$. Let $\mathcal{O}$ be the region covered by the elements of $\widetilde{\mathcal{T}}$, i.e., let $\mathcal{O}=\widetilde{S}$ if $\widetilde{\mathcal{T}}$ is a reference patch, $\mathcal{O}=\widetilde{T}$ if $\widetilde{\mathcal{T}} \in \{\widetilde{\mathcal{T}}^{\mathsf{C},\mathrm{half},n}_{geo,\sigma}, \widetilde{\mathcal{T}}^{\mathsf{M},\mathrm{half},L,n}_{geo,\sigma}\}$ is a reference half-patch and $\mathcal{O}=\widetilde{T}^{\mathrm{flip}}$ if $\widetilde{\mathcal{T}} = \widetilde{\mathcal{T}}^{\mathsf{C},\mathrm{half,flip},n}_{geo,\sigma}$. Let $\widetilde{u}$ be analytic on $\overline{\mathcal{O}}$ and assume there exist constants $\varepsilon\in(0,1]$, $\beta\in[0,1)$, γ, $C_u>0$ such that for all $p\in\mathbb{N}_0$ and all $\widetilde{\mathbf{x}}\in\widetilde{S}$

$$|\nabla^p(\widetilde{u}(\widetilde{\mathbf{x}})-\widetilde{u}(\mathbf{0}))| \le C_u\varepsilon^{-1}\gamma^p(\widetilde{r}(\widetilde{\mathbf{x}})/\varepsilon)^{1-\beta}\widetilde{r}(\widetilde{\mathbf{x}})^{-p}\max\{p+1,\widetilde{r}(\widetilde{\mathbf{x}})/\varepsilon\}^{p+1}\ . \tag{3.8}$$

Then, there are constants C, b, $\kappa>0$ depending only on γ, σ, and β (in particular, independent of ε, n, L) such that under the scale resolution condition

$$q\varepsilon \ge \kappa \tag{3.9}$$

there holds

$$\|\widetilde{u}-\widetilde{\Pi}_q\widetilde{u}\|_{L^\infty(\mathcal{O})} + \|\nabla(\widetilde{u}-\widetilde{\Pi}_q\widetilde{u})\|_{L^2(\mathcal{O})} \le CC_u\left(q^9\sigma^{n(1-\beta)}+e^{-bq}\right). \tag{3.10}$$

(ii) Let $\widetilde{\mathcal{T}} \in \{\widetilde{\mathcal{T}}^{\mathsf{BL},L}, \widetilde{S}\}$. Let $\widetilde{u}$ be analytic on $\widetilde{S}$ and assume that there are constants C_u, $\gamma>0$ such that for every $p\in\mathbb{N}_0$

$$\|\nabla^p\widetilde{u}\|_{L^\infty(\widetilde{S})} \le C_u\gamma^p\max\{p+1,\varepsilon^{-1}\}^{p+1}. \tag{3.11}$$

Then there are constants C, b, $\kappa > 0$ depending only on γ and σ (in particular, they are independent of ε and L) such that under the constraint (3.9) there holds

$$\|\widetilde{u} - \widetilde{\Pi}_q \widetilde{u}\|_{W^{1,\infty}(\widetilde{S})} \le C C_u e^{-bq}. \tag{3.12}$$

Proof. Proof of (i): Step 1: Elements abutting on $\mathbf{0}$: Only triangles $\triangle$ may abutt on $\mathbf{0}$. Let $\widetilde{K}$ be such a triangle. From (3.8) and estimating (generously) $\max\{1, \widetilde{r}(\cdot)/\varepsilon\}^3 \lesssim \varepsilon^{-3}$, we get the existence of $C > 0$ independent of $\varepsilon \in (0,1]$ with

$$\forall \widetilde{\mathbf{x}} \in \widetilde{K}: \quad |\nabla^2 \widetilde{u}(\widetilde{\mathbf{x}})| \le C(\widetilde{r}(\widetilde{\mathbf{x}}))^{-1-\beta} \varepsilon^{-5+\beta}. \tag{3.13}$$

By scaling this bound and invoking Lemma 3.1, (iv), we get with $h_{\widetilde{K}} := \operatorname{diam} \widetilde{K}$ for any fixed $\widetilde{\beta} \in (\beta, 1)$

$$\begin{aligned} \|\widetilde{u} - \widetilde{\Pi}_q \widetilde{u}\|_{L^\infty(\widetilde{K})} + \|\nabla(\widetilde{u} - \widetilde{\Pi}_q \widetilde{u})\|_{L^2(\widetilde{K})} &\le C q^4 h_{\widetilde{K}}^{1-\widetilde{\beta}} \|\widetilde{r}^{\widetilde{\beta}} \nabla^2 \widetilde{u}\|_{L^2(\widetilde{K})} \\ &\overset{(3.13)}{\le} C q^4 h_{\widetilde{K}}^{1-\widetilde{\beta}} \varepsilon^{-5+\beta} h_{\widetilde{K}}^{\widetilde{\beta}-\beta} \overset{q\varepsilon \ge \kappa}{\le} C q^{4+5-\beta} h_{\widetilde{K}}^{1-\beta} \lesssim q^{9-\beta} \sigma^{n(1-\beta)}. \end{aligned} \tag{3.14}$$

Step 2: Elements not abutting on $\mathbf{0}$: From Lemma 2.8, (v) we get $\widetilde{r}(\cdot) \lesssim h_{\widetilde{K}} = \operatorname{diam} \widetilde{K}$ on $\widetilde{K}$. The regularity assumption (3.8) then implies that there exist (suitably adjusted) constants C, γ such that for all $p \in \mathbb{N}_0$

$$\|\nabla^p(\widetilde{u} - \widetilde{u}(\mathbf{0}))\|_{L^\infty(\widetilde{K})} \le C \gamma^p \varepsilon^{-3+\beta} h_{\widetilde{K}}^{1-\beta} \widetilde{r}^{-p} \max\{p+1, \varepsilon^{-1}\}^p . \tag{3.15}$$

We now consider the approximation on triangles and rectangles separately.

Step 2.1: $\widetilde{K}$ is a triangle $\triangle$. Lemma 2.8, (ii) implies in particular that $h_{\widetilde{K}} \lesssim \widetilde{r}(\cdot)$ on $\widetilde{K}$. Scaling the bounds (3.15) to the reference element $\widehat{K} = \widehat{T}$ therefore gives for $\widehat{u} := \widetilde{u} \circ A_{\widetilde{K}}$, where $A_{\widetilde{K}} : \widehat{K} \to \widetilde{K}$ is the affine element map for $\widetilde{K}$, the existence of constants C, $\gamma > 0$ such that

$$\forall p \in \mathbb{N}_0: \quad \|\widehat{\nabla}^p(\widehat{u} - \widehat{u}(\mathbf{0}))\|_{L^\infty(\widehat{K})} \le C \gamma^p \varepsilon^{-3+\beta} h_{\widetilde{K}}^{1-\beta} \max\{p+1, \varepsilon^{-1}\}^p . \tag{3.16}$$

In order to be able to apply the approximation properties of Lemma 3.1, we note

$$\begin{aligned} \max\{p+1, \varepsilon^{-1}\}^p &= \max\{(p+1)^p, \varepsilon^{-p}(p+1)^{-p}(p+1)^p\} \\ &= (p+1)^p \max\{1, \varepsilon^{-p}(p+1)^{-p}\} \le (p+1)^p \max\{1, \frac{(1/\varepsilon)^p}{p!}\} \\ &\le (p+1)^p e^{1/\varepsilon} \overset{q\varepsilon \ge \kappa}{\le} (p+1)^p e^{q/\kappa}. \end{aligned} \tag{3.17}$$

Inserting (3.17) into (3.16) yields that there are constants $C > 0$, $\gamma > 0$ such that

$$\forall p \in \mathbb{N}_0: \quad \|\nabla^p(\widehat{u} - \widehat{u}(\mathbf{0}))\|_{L^\infty(\widehat{K})} \le C e^{q/\kappa} \varepsilon^{-3+\beta} h_{\widetilde{K}}^{1-\beta} \gamma^p (p+1)^p. \tag{3.18}$$

We are in a position to apply Lemma 3.1. The parameter δ in (3.1) is determined by γ. In view of $q\varepsilon \ge \kappa$, we can ensure condition (3.1) by selecting κ sufficiently large to obtain from Lemma 3.1 with a $b > 0$ depending only on γ

$$\|\widehat{u} - \widehat{\Pi}_q^{\triangle} \widehat{u}\|_{W^{1,\infty}(\widehat{K})} \le C h_{\widetilde{K}}^{1-\beta} e^{q/\kappa} \varepsilon^{-3+\beta} e^{-bq},$$

We may assume that κ is so large that $1/\kappa - b \le -b/2$ to absorb $e^{q/\kappa}$. Finally, in view of $q\varepsilon \ge \kappa$, we can also absorb the factor $\varepsilon^{-3+\beta} \lesssim q^{3-\beta}$ in the exponentially decaying one by adjusting b. Upon scaling from $\widehat{K}$ to $\widetilde{K}$ we get the existence of constants b, $C > 0$ such that

$$\forall q \in \mathbb{N}: \quad \|\widetilde{u} - \widetilde{\Pi}_q \widetilde{u}\|_{L^\infty(\widetilde{K})} + \|\nabla(\widetilde{u} - \widetilde{\Pi}_q \widetilde{u})\|_{L^2(\widetilde{K})} \le C h_{\widetilde{K}}^{1-\beta} e^{-bq}. \tag{3.19}$$

Step 2.2: $\widetilde{K}$ is a rectangle $\square$. We argue as in the case of a triangle in Step 2.1. Starting point is again the regularity assertion (3.8). The rectangle $\widetilde{K}$ has side lengths $h_{\widetilde{K},\widetilde{y}} \le h_{\widetilde{K},\widetilde{x}} \le 1$. From Lemma 2.8, (iv) we have $h_{\widetilde{K},\widetilde{y}} \le h_{\widetilde{K},\widetilde{x}} \le C\widetilde{r}(\cdot)$ on $\widetilde{K}$. Hence, the (anisotropic) scaling to the reference square $\widehat{S}$ of the estimates (3.8) yields, for all $(n,m) \in \mathbb{N}_0^2$, in view of (3.17)

$$\begin{aligned} \|\partial_x^m \partial_y^n (\widehat{u} - \widehat{u}(\mathbf{0}))\|_{L^\infty(\widehat{S})} &\le C\varepsilon^{-3+\beta} h_{\widetilde{K},\widetilde{x}}^{1-\beta} \gamma^{n+m} h_{\widetilde{K},\widetilde{x}}^m h_{\widetilde{K},\widetilde{y}}^n h_{\widetilde{K},\widetilde{x}}^{-(n+m)} e^{q/\kappa} (n+m)^{n+m} \\ &\overset{(B.9)}{\le} \varepsilon^{-3+\beta} h_{\widetilde{K},\widetilde{x}}^{1-\beta} \gamma^{n+m} e^{q/\kappa} n!m!, \end{aligned} \tag{3.20}$$

where we again possibly adjusted the value of γ. Lemma 3.2 (with $h_y = h_{\widetilde{K},\widetilde{y}}/h_{\widetilde{K},\widetilde{x}} \le 1$ and $\varepsilon_x = \varepsilon_y = 1$ there) yields with the regularity estimates (3.20) the existence of constants C, $b > 0$ such that for all $q \in \mathbb{N}_0$

$$\begin{aligned} \|\widehat{u} - \widehat{\Pi}_q^\square \widehat{u}\|_{L^\infty(\widehat{K})} + \|\partial_{\widehat{x}}(\widehat{u} - \widehat{\Pi}_q^\square \widehat{u})\|_{L^\infty(\widehat{K})} &\le C\varepsilon^{-3+\beta} h_{\widetilde{K},\widetilde{x}}^{1-\beta} e^{-bq}, \\ \|\partial_{\widehat{y}}(\widehat{u} - \widehat{\Pi}_q^\square \widehat{u})\|_{L^\infty(\widehat{K})} &\le C\varepsilon^{-3+\beta} h_{\widetilde{K},\widetilde{x}}^{1-\beta} \frac{h_{\widetilde{K},\widetilde{y}}}{h_{\widetilde{K},\widetilde{x}}} e^{-bq}, \end{aligned}$$

where the factor $e^{q/\kappa}$ was absorbed again in the exponentially decaying term by taking κ sufficiently large. We obtain on $\widetilde{S}$

$$\begin{aligned} \|\partial_{\widetilde{x}}(\widetilde{u} - \widetilde{\Pi}_q \widetilde{u})\|_{L^2(\widetilde{S})} &\le C\varepsilon^{-3+\beta} \sqrt{h_{\widetilde{K},\widetilde{x}} h_{\widetilde{K},\widetilde{y}}}\, h_{\widetilde{K},\widetilde{x}}^{-1} h_{\widetilde{K},\widetilde{x}}^{1-\beta} e^{-bq} \\ &\overset{q\varepsilon \ge \kappa}{\le} C\sqrt{h_{\widetilde{K},\widetilde{y}}/h_{\widetilde{K},\widetilde{x}}}\, h_{\widetilde{K},\widetilde{x}}^{1-\beta} e^{-bq}, \end{aligned} \tag{3.21a}$$

$$\|\partial_{\widetilde{y}}(\widetilde{u} - \widetilde{\Pi}_q \widetilde{u})\|_{L^2(\widetilde{S})} \le C\sqrt{h_{\widetilde{K},\widetilde{y}}/h_{\widetilde{K},\widetilde{x}}}\, h_{\widetilde{K},\widetilde{x}}^{1-\beta} e^{-bq}, \tag{3.21b}$$

$$\|(\widetilde{u} - \widetilde{\Pi}_q \widetilde{u})\|_{L^\infty(\widetilde{S})} \le C h_{\widetilde{K},\widetilde{x}}^{1-\beta} e^{-bq}, \tag{3.21c}$$

where again we adjusted the values of the constants b, C in both estimates to absorb algebraic factors in q.

Step 3: Summation of the elemental errors: We note that the element size $h_{\widetilde{K}}$ of the elements abutting on $\mathbf{0}$ is $h_{\widetilde{K}} \sim \sigma^n$. For the finitely many contributions from the (triangular) elements $\widetilde{K}$ touching $\mathbf{0}$ we have by (3.14) the existence of $C > 0$ such that for every $q \ge 1$

$$\sum_{\widetilde{K}\,:\,\mathbf{0} \in \overline{\widetilde{K}}} \|\widetilde{u} - \widetilde{\Pi}_q \widetilde{u}\|_{H^1(\widetilde{K})}^2 \overset{(3.14)}{\le} C q^{18} \sigma^{2n(1-\beta)}.$$

The sum of squared error contributions over all triangular elements not touching $\mathbf{0}$ is also bounded by e^{-2bq} by combining (3.19) and Lemma 2.8, (vi). Likewise, the sum

over all rectangular elements is bounded by e^{-2bq} by combining (3.21) and Lemma 2.8, (vii).

Proof of (ii): The proof is similar to the proof of case (i) and can be obtained from it by formally setting $\beta = 0$ and $\widetilde{r} \equiv 1$ and dropping the error contribution $q^8\sigma^{n(1-\beta)}$ which is due to the small elements touching $\mathbf{0}$. ∎

3.2.2. *hp*-FE approximation of boundary layer functions.

Lemma 3.4 (approximation of boundary layer functions). *Fix $c_1 > 0$.*

(i) Let $\widetilde{\mathcal{T}} \in \{\widetilde{\mathcal{T}}^{\mathsf{M},\mathrm{half},L,n}_{geo,\sigma}, \widetilde{\mathcal{T}}^{\mathsf{BL},L}_{geo,\sigma}\}$. Let $\widetilde{\mathcal{T}}' \subset \widetilde{\mathcal{T}}$ and let $\mathcal{O} := \mathrm{interior}\big(\cup\{\overline{\widetilde{K}} \mid \widetilde{K} \in \widetilde{\mathcal{T}}'\}\big)$ be the union of the elements of $\widetilde{\mathcal{T}}'$. Let $\widetilde{u}$ be analytic on $\mathcal{O}$ and satisfy for some C_u, γ, $\alpha > 0$, $\varepsilon \in (0,1]$ and for all $(m,n) \in \mathbb{N}_0^2$ and all $\widetilde{\mathbf{x}} = (\widetilde{x}, \widetilde{y}) \in \mathcal{O}$

$$|\partial_{\widetilde{x}}^m \partial_{\widetilde{y}}^n \widetilde{u}(\widetilde{\mathbf{x}})| \le C_u \gamma^{n+m} m! \max\{n, \varepsilon^{-1}\}^n e^{-\alpha\widetilde{y}/\varepsilon}. \tag{3.22}$$

Assume that L is such that the scale resolution condition

$$\sigma^L \le c_1 \varepsilon \tag{3.23}$$

is satisfied. Then there are constants C, $b > 0$ depending only on γ, α, c_1, σ such that

$$\forall q \in \mathbb{N}\colon \quad \|\widetilde{u} - \widetilde{\Pi}_q \widetilde{u}\|_{L^\infty(\mathcal{O})} + \varepsilon \|\nabla(\widetilde{u} - \widetilde{\Pi}_q \widetilde{u})\|_{L^\infty(\mathcal{O})} \le C C_u e^{-bq}. \tag{3.24}$$

(ii) Let $\widetilde{\mathcal{T}}'' \subset \widetilde{\mathcal{T}}^{\mathsf{C},\mathrm{half},n}_{geo,\sigma}$ or $\widetilde{\mathcal{T}}'' \subset \widetilde{\mathcal{T}}^{\mathsf{C},\mathrm{half,flip},n}_{geo,\sigma}$. Let $\mathcal{O} := \mathrm{interior}\big(\cup\{\overline{\widetilde{K}} \mid \widetilde{K} \in \widetilde{\mathcal{T}}''\}\big)$ be the union of the elements of $\widetilde{\mathcal{T}}''$. Let $\widetilde{u}$ be analytic on $\mathcal{O}$ and satisfy for some C_u, γ, $\alpha > 0$, $\varepsilon \in (0,1]$

$$\forall p \in \mathbb{N}_0 \ \forall \widetilde{\mathbf{x}} \in \mathcal{O}\colon \quad |\nabla^p \widetilde{u}(\widetilde{\mathbf{x}})| \le C_u \gamma^p \max\{p, \varepsilon^{-1}\}^p e^{-\alpha\widetilde{r}(\widetilde{\mathbf{x}})/\varepsilon}. \tag{3.25}$$

Assume that n is such that $c_1 > 0$, $n \in \mathbb{N}$ satisfies the scale scale resolution condition

$$\sigma^n \le c_1 \varepsilon \tag{3.26}$$

is satisfied. Then, there are constants C, $b > 0$ (depending only on γ, α, c_1, σ) such that

$$\forall q \in \mathbb{N}\colon \quad \|\widetilde{u} - \widetilde{\Pi}_q \widetilde{u}\|_{L^\infty(\mathcal{O})} + \varepsilon \|\nabla(\widetilde{u} - \widetilde{\Pi}_q \widetilde{u})\|_{L^\infty(\mathcal{O})} \le C C_u e^{-bq}. \tag{3.27}$$

Proof. Proof of (ii): We only consider the case $\mathcal{T}'' \subset \widetilde{\mathcal{T}}^{\mathsf{C},\mathrm{half},n}_{geo,\sigma}$ as the case $\mathcal{T}'' \subset \widetilde{\mathcal{T}}^{\mathsf{C},\mathrm{half,flip},n}_{geo,\sigma}$ is handled similarly. We note that the patch $\widetilde{\mathcal{T}}^{\mathsf{C},\mathrm{half},n}_{geo,\sigma}$ consists of triangles only, which are all shape-regular. Let $\widetilde{K} \subset \mathcal{O}$ be a triangle and let $h_{\widetilde{K}} = \mathrm{diam}\, \widetilde{K}$. In the case that $\widetilde{K}$ touches $\mathbf{0}$, the condition (3.26) implies that $h_{\widetilde{K}} \lesssim \sigma^n \lesssim c_1\varepsilon$ so that

$$\frac{h_{\widetilde{K}}}{q\varepsilon} \lesssim \frac{1}{q}. \tag{3.28}$$

Hence, for every fixed choice of the constant c_1 there exists $q_0 = q_0(c_1) \in \mathbb{N}$ (independent of ε) such that for every $q \ge q_0$ one has the scale resolution condition (3.1). Then, Lemma 3.1, (v) implies for suitable $b > 0$ (independent of ε)

$$\|\widetilde{u} - \widetilde{\Pi}_q \widetilde{u}\|_{L^\infty(\widetilde{K})} + \varepsilon \|\nabla(\widetilde{u} - \widetilde{\Pi}_q \widetilde{u})\|_{L^\infty(\widetilde{K})} \lesssim e^{-bq}. \tag{3.29}$$

If $\widetilde{K}$ does not touch $\mathbf{0}$, we distinguish between two further cases. In the first case, we assume that $h_{\widetilde{K}}/(q\varepsilon) \le \delta$ and proceed as above: The scale resolution condition (3.1) is satisfied, and we arrive again at (3.29). In the case $h_{\widetilde{K}}/(q\varepsilon) \ge \delta$, we note that Lemma 2.8, (ii) implies $\operatorname{dist}(\widetilde{K}, \mathbf{0}) \ge c_2 h_{\widetilde{K}} \ge c_2 \delta q \varepsilon$. Hence, by the decay properties of $\widetilde{u}$ in (3.25) we have

$$\|\widetilde{u}\|_{L^\infty(\widetilde{K})} + \varepsilon \|\nabla \widetilde{u}\|_{L^\infty(\widetilde{K})} \le C e^{-\alpha c_2 h_{\widetilde{K}}/\varepsilon} \le C e^{-\alpha c_2 q \delta}. \tag{3.30}$$

In view of the stability properties (3.7), we conclude

$$\|\widetilde{u} - \widetilde{\Pi}_q \widetilde{u}\|_{L^\infty(\widetilde{K})} + \varepsilon \|\nabla(\widetilde{u} - \widetilde{\Pi}_q \widetilde{u})\|_{L^\infty(\widetilde{K})} \lesssim e^{-bq}. \tag{3.31}$$

<u>Proof of (i):</u> We distinguish between triangular and rectangular elements.

<u>Approximation of $\widetilde{u}$ on triangular elements $\widetilde{K}$:</u> Triangular elements do not appear in boundary layer patches $\widetilde{\mathcal{T}}^{\mathsf{BL},L}_{geo,\sigma}$ but only in $\widetilde{\mathcal{T}}^{\mathsf{M},\mathrm{half},L,n}_{geo,\sigma}$. For patches $\widetilde{\mathcal{T}}^{\mathsf{M},\mathrm{half},L,n}_{geo,\sigma}$ inspection (cf. Fig. 2.2) shows that two types of triangles occur: the first type are the triangles $\widetilde{K}$ in $\widetilde{T} \setminus \widetilde{T}_1$ on which one has $\widetilde{r}(\widetilde{x}, \widetilde{y}) \sim \widetilde{y}$ (uniformly in L, n). The second type are the triangles in $\widetilde{T}_1$. For the first type, we have from (3.22) the regularity assertion (with suitably adjusted C_u, γ, α independent of ε)

$$\forall \widetilde{\mathbf{x}} \in \widetilde{K}\ \forall n \in \mathbb{N}_0 : \quad |\nabla^n \widetilde{u}(\widetilde{\mathbf{x}})| \le C_u \gamma^n \max\{n, \varepsilon^{-1}\}^n e^{-\alpha \widetilde{r}(\widetilde{\mathbf{x}})/\varepsilon}.$$

This is the same regularity assumption that underlies the proof of part (ii) of the lemma so that the same arguments can be brought to bear as in the case of part (ii). For the second type of triangles, i.e., $\widetilde{K} \subset \widetilde{T}_1 \subset (0, \sigma^L)^2$, the resolution assumption (3.23) implies for the element size $h_{\widetilde{K}} \lesssim \sigma^L \lesssim \varepsilon$. Hence, again Lemma 3.1, (v) is applicable and yields the desired exponential approximation.

<u>Approximation of $\widetilde{u}$ on rectangular elements $\widetilde{K}$:</u> The case of rectangular elements $\widetilde{K}$ with side lengths $h_{\widetilde{K},x}$, $h_{\widetilde{K},y}$ is similar to the case of triangles. We note that the patches $\widetilde{\mathcal{T}}^{\mathsf{BL},L}_{geo,\sigma}$ and $\widetilde{\mathcal{T}}^{\mathsf{M},\mathrm{half},L,n}_{geo,\sigma}$ are such that $h_{\widetilde{K},\widetilde{y}} \le h_{\widetilde{K},\widetilde{x}} \le 1$. The anisotropic scaling from $\widetilde{K}$ to $\widehat{K}$ and the regularity assumption (3.22) show that the pull-back $\widehat{u}$ to $\widehat{K}$ satisfies for all $(m, n) \in \mathbb{N}_0^2$

$$\|\partial_{\widehat{x}}^m \partial_{\widehat{y}}^n \widehat{u}\|_{L^\infty(\widehat{K})} \le C e^{-\alpha \operatorname{dist}(\widetilde{K}, \{\widetilde{y}=0\})/\varepsilon} h_{\widetilde{K},\widetilde{x}}^m h_{\widetilde{K},\widetilde{y}}^n \gamma^{n+m} m! \max\{n+1, \varepsilon^{-1}\}^n .$$

That is, $\widehat{u}$ satisfies the analytic regularity condition (3.2) with $\varepsilon_y = \varepsilon$, $\varepsilon_x = 1$, $h_x = h_{\widetilde{K},\widetilde{x}}$, $h_y = h_{\widetilde{K},\widetilde{y}}$ and $C_u = C e^{-\alpha \operatorname{dist}(\widetilde{K}, \{\widetilde{y}=0\})/\varepsilon}$. We observe that the resolution condition (3.3) can be achieved if $\widetilde{K}$ touches the line $\{\widetilde{y} = 0\}$ in view of (3.23) provided that $q \ge q_0 \ge 1$ for suitable q_0 (depending on c_1, σ, γ). If $\widetilde{K}$ does not touch the line $\{\widetilde{y} = 0\}$, then two cases may occur: If the resolution condition (3.3) is still satisfied then we obtain again exponential convergence. If not, we note that $h_{\widetilde{K},\widetilde{y}} \le h_{\widetilde{K},\widetilde{x}}$ and that we may assume $h_{\widetilde{K},\widetilde{x}}/q \le \delta/2$ by assuming $q \ge q_0 \ge 1$ (note: trivially, $h_{\widetilde{K},\widetilde{x}} \le 1$ so that $q_0 \ge 2/\delta$ will work). Furthermore, Lemma 2.8, (iii) reveals again that $\operatorname{dist}(\widetilde{K}, \{\widetilde{y} = 0\}) \ge c_3 h_{\widetilde{K},\widetilde{y}}$; since $h_{\widetilde{K},\widetilde{y}}/(\varepsilon q) \ge \delta/2$ we get $\operatorname{dist}(\widetilde{K}, \{\widetilde{y} = 0\})/\varepsilon \ge q c_3 \delta/2$. Hence, $\exp(-\alpha \operatorname{dist}(\widetilde{K}, \{\widetilde{y} = 0\})/\varepsilon) \le \exp(-q \alpha c_2 \delta/2)$ and we may argue as in the case of triangles that $\widetilde{u}$ is exponentially (in q) small on $\widetilde{K}$. The stability of $\widetilde{\Pi}_q$ given in (3.7) then concludes the argument. ∎

3.2.3. *hp*-FE approximation of corner layer functions.

Lemma 3.5 (approximation of corner layer functions). *Fix $c_1 > 0$. Let $\widetilde{\mathcal{T}} \in \{\widetilde{\mathcal{T}}^{\mathsf{M},\mathrm{half},L,n}_{geo,\sigma}, \widetilde{\mathcal{T}}^{\mathsf{C},\mathrm{half},n}_{geo,\sigma}, \widetilde{\mathcal{T}}^{\mathsf{C},\mathrm{half},\mathrm{flip},n}_{geo,\sigma}, \widetilde{\mathcal{T}}^{\mathsf{C},n}_{geo,\sigma}, \widetilde{\mathcal{T}}^{\mathsf{T},n}_{geo,\sigma}\}$. Let $\widetilde{\mathcal{T}}' \subset \widetilde{\mathcal{T}}$ and let $\mathcal{O} := \mathrm{interior}\big(\cup\{\overline{\widetilde{K}} \mid \widetilde{K} \in \widetilde{\mathcal{T}}'\}\big)$ be the union of the elements of $\widetilde{\mathcal{T}}'$. Let $\widetilde{u}$ be analytic on $\mathcal{O}$ and satisfy for some $\beta \in [0,1)$, $\varepsilon \in (0,1]$, C_u, γ, $\alpha > 0$*

$$\forall \widetilde{\mathbf{x}} \in \mathcal{O} \quad \forall p \in \mathbb{N}_0 : \quad |\nabla^p \widetilde{u}(\widetilde{\mathbf{x}})| \le C_u \varepsilon^{\beta-1} \gamma^p (\widetilde{r}(\widetilde{\mathbf{x}}))^{1-\beta-p} p! e^{-\alpha \widetilde{r}(\widetilde{\mathbf{x}})/\varepsilon}. \tag{3.32}$$

Assume that $n \in \mathbb{N}$ is such that the scale resolution condition

$$\sigma^n \le c_1 \varepsilon. \tag{3.33}$$

is satisfied. Then there are constants C, $b > 0$ depending only on γ, α, c_1, σ, and β (in particular, they are independent of ε, q, n, L) such that for all $q \in \mathbb{N}$

$$\|\widetilde{u} - \widetilde{\Pi}_q \widetilde{u}\|_{L^\infty(\mathcal{O})} \le C C_u \left(e^{-bq} + q^4 \varepsilon^{\beta-1} \sigma^{n(1-\beta)} \right), \tag{3.34}$$

$$\|\widetilde{u} - \widetilde{\Pi}_q \widetilde{u}\|_{L^2(\mathcal{O})} + \varepsilon \|\nabla(\widetilde{u} - \widetilde{\Pi}_q \widetilde{u})\|_{L^2(\mathcal{O})} \le C C_u \varepsilon \left(e^{-bq} + q^4 \varepsilon^{\beta-1} \sigma^{n(1-\beta)} \right). \tag{3.35}$$

In the estimates (3.34), (3.35) the term $q^4 \varepsilon^{\beta-1} \sigma^{n(1-\beta)}$ can be dropped if $\mathcal{O}$ does not touch $\mathbf{0}$.

Proof. The approximation of functions of corner layer type $\widetilde{u}$ proceeds structurally along the same lines as in the case of the singularity functions in Lemma 3.3. We distinguish between the elements touching $\mathbf{0}$ and the remaining ones.

<u>$\widetilde{K}$ touches $\mathbf{0}$</u>: Selecting $\widetilde{\beta} \in (\beta, 1)$ we obtain by arguing as in (3.14)

$$\begin{aligned} \|\widetilde{u} - \widetilde{\Pi}_q \widetilde{u}\|_{L^\infty(\widetilde{K})} + \|\nabla(\widetilde{u} - \widetilde{\Pi}_q \widetilde{u})\|_{L^2(\widetilde{K})} &\lesssim h_{\widetilde{K}}^{1-\widetilde{\beta}} q^4 \|\widetilde{r}^{\widetilde{\beta}} \nabla^2 \widetilde{u}\|_{L^2(\widetilde{K})} \\ &\lesssim q^4 (h_{\widetilde{K}}/\varepsilon)^{1-\beta}. \end{aligned} \tag{3.36}$$

Since $h_{\widetilde{K}} \lesssim \sigma^n$ for elements $\widetilde{K}$ touching $\mathbf{0}$, their contributions lead to the term $q^4 \varepsilon^{\beta-1} \sigma^{n(1-\beta)}$.

<u>K does not touch $\mathbf{0}$</u>: We distinguish between triangular and rectangular elements.

<u>Step 1: $\widetilde{K}$ is a triangular element:</u> As in the case of the approximation in Lemma 3.3, we get from Lemma 3.1, (v) and scaling that (for suitably adjusted C, α)

$$\|\widetilde{u} - \widetilde{\Pi}_q \widetilde{u}\|_{L^\infty(\widetilde{K})} + \|\nabla(\widetilde{u} - \widetilde{\Pi}_q \widetilde{u})\|_{L^2(\widetilde{K})} \le C (h_{\widetilde{K}}/\varepsilon)^{1-\beta} e^{-bq} e^{-\alpha h_{\widetilde{K}}/\varepsilon}. \tag{3.37}$$

<u>Step 2: $\widetilde{K}$ is a rectangular element:</u> We recall $h_{\widetilde{K},\widetilde{y}} \le h_{\widetilde{K},\widetilde{x}} \le 1$. By Lemma 2.8, (iv) we have $\widetilde{r}(\cdot) \sim h_{\widetilde{K},\widetilde{x}}$ on $\widetilde{K}$. As in the case of Lemma 3.3 we observe for the pull-back to the reference element $\widehat{K}$

$$\forall (m,n) \in \mathbb{N}_0^2 : \quad \|\partial_{\widetilde{x}}^m \partial_{\widetilde{y}}^n \widehat{u}\|_{L^\infty(\widehat{K})} \le C (h_{\widetilde{K},\widetilde{x}}/\varepsilon)^{1-\beta} e^{-\alpha h_{\widetilde{K},\widetilde{x}}/\varepsilon} \gamma^{n+m} n! m! h_{\widetilde{K},\widetilde{x}}^{m-(m+n)} h_{\widetilde{K},\widetilde{y}}^n.$$

Using Lemma 3.2, (iv) (with $\varepsilon_x = \varepsilon_y = 1$ and $h_y = h_{\widetilde{K},\widetilde{y}}/h_{\widetilde{K},\widetilde{x}}$, $h_x = 1$ there), we arrive at

$$\|\widehat{u} - \widehat{\Pi}_q^{\square} \widehat{u}\|_{L^\infty(\widehat{K})} \le C (h_{\widetilde{K}}/\varepsilon)^{1-\beta} e^{-bq} e^{-\alpha h_{\widetilde{K},\widetilde{x}}/\varepsilon}, \tag{3.38}$$

$$\|\partial_{\widetilde{x}} (\widehat{u} - \widehat{\Pi}_q^{\square} \widehat{u})\|_{L^\infty(\widehat{K})} \le C (h_{\widetilde{K}}/\varepsilon)^{1-\beta} e^{-bq} e^{-\alpha h_{\widetilde{K},\widetilde{x}}/\varepsilon}, \tag{3.39}$$

$$\|\partial_{\widetilde{y}} (\widehat{u} - \widehat{\Pi}_q^{\square} \widehat{u})\|_{L^\infty(\widehat{K})} \le C (h_{\widetilde{K}}/\varepsilon)^{1-\beta} \frac{h_{\widetilde{K},\widetilde{y}}}{h_{\widetilde{K},\widetilde{x}}} e^{-bq} e^{-\alpha h_{\widetilde{K},\widetilde{x}}/\varepsilon}. \tag{3.40}$$

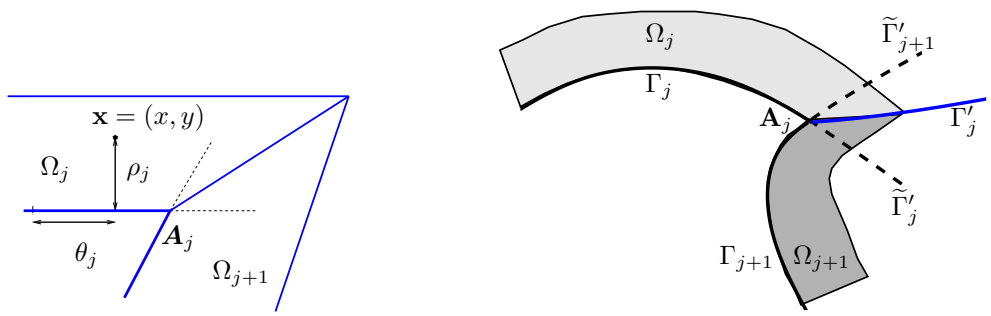

FIG. 4.1. *Left: boundary fitted coordinates $\psi_j : (\rho_j, \theta_j) \mapsto (x, y)$. Right: typical situation at a reentrant corner: boundary fitted coordinates (ρ_j, θ_j) and $(\rho_{j+1}, \theta_{j+1})$ are valid in the regions Ω_j, Ω_{j+1}, respectively. $\widetilde{\Gamma}_j$ and $\widetilde{\Gamma}_{j+1}$ are analytic continuations of Γ_j, Γ_{j+1}. The analytic arc Γ'_j is such that the angles $\angle(\Gamma'_j, \Gamma_j)$ and $\angle(\Gamma_{j+1}, \Gamma'_j)$ are both less than π.*

Step 3 (L^∞-bound): Since $\sup_{t>0} t^{1-\beta} e^{-t} < \infty$, the L^∞-estimates follow easily from (3.36), (3.37) (3.38).

Step 4 (energy norm estimate): Proceeding as in Step 3 of the proof of Lemma 3.3 we set $e_{\widetilde{K}} := \widetilde{u} - \widetilde{\Pi}_q \widetilde{u}$ and get, using $h_{\widetilde{K}} \lesssim \varepsilon$ for the elements abutting on $\mathbf{0}$:

$$\begin{aligned} &\sum_{\widetilde{K}\colon \widetilde{K} \text{ abutts on } \mathbf{0}} \|e_{\widetilde{K}}\|^2_{L^2(\widetilde{K})} + \varepsilon^2 \|\nabla e_{\widetilde{K}}\|^2_{L^2(\widetilde{K})} \\ &\overset{(3.36)}{\lesssim} q^8 \sum_{\widetilde{K}\colon \widetilde{K} \text{ abutts on } \mathbf{0}} (h^2_{\widetilde{K}} + \varepsilon^2)(h_{\widetilde{K}}/\varepsilon)^{2(1-\beta)} \lesssim q^8 \varepsilon^{2\beta} \sigma^{2n(1-\beta)}. \end{aligned}$$

For the remaining elements, we consider the triangular elements and the rectangular ones. In both cases, we employ the simple observation

$$\|e_{\widetilde{K}}\|_{L^2(\widetilde{K})} \lesssim h_{\widetilde{K}} \|e_{\widetilde{K}}\|_{L^\infty(\widetilde{K})} = \varepsilon \frac{h_{\widetilde{K}}}{\varepsilon} \|e_{\widetilde{K}}\|_{L^\infty(\widetilde{K})}. \tag{3.41}$$

The sum over all triangles, collected in $\widetilde{\mathcal{T}}^\triangle$, yields by combining (3.37) and (3.41) with Lemma 2.8, (viii)

$$\sum_{\widetilde{K} \in \widetilde{\mathcal{T}}^\triangle} \|e_{\widetilde{K}}\|^2_{L^2(\widetilde{K})} + \varepsilon^2 \|e_{\widetilde{K}}\|^2_{H^1(\widetilde{K})} \lesssim \varepsilon^2 e^{-2bq}.$$

Likewise, the sum over all rectangular elements, collected in $\widetilde{\mathcal{T}}^\square$, yields by combining Lemma 2.8, (ix) with (3.38), (3.41) for the L^2-part and with (3.39), (3.40) for the H^1-part

$$\sum_{\widetilde{K} \in \widetilde{\mathcal{T}}^\square} \|e_{\widetilde{K}}\|^2_{L^2(\widetilde{K})} + \varepsilon^2 \|e_{\widetilde{K}}\|^2_{H^1(\widetilde{K})} \lesssim \varepsilon^2 e^{-2bq}.$$

This concludes the proof. ∎

4. *hp*-FE approximation of singularly perturbed problems on geometric boundary layer meshes. The principal result of the present paper is a robust, exponential approximation result for solutions of the singular perturbation problem (1.1), (1.2) in curvilinear polygonal domains from spaces based on geometric boundary layer meshes that are able to resolve the length scales present in the problem. The meshes are independent of ε but subject to the (weak) scale resolution condition (4.1).

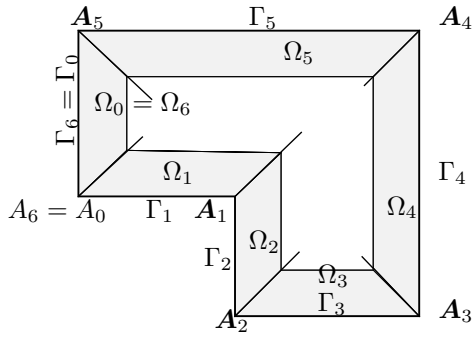

Fig. 4.2. *The subdomains Ω_j on which the boundary layer expansion $u_\varepsilon^{\mathsf{BL}}$ is defined in terms of boundary fitted coordinates (ρ_j, θ_j).*

Theorem 4.1. *Let the Lipschitz domain $\Omega \subset \mathbb{R}^2$ be a curvilinear polygon with J vertices as described in Section 1.2. Let A, c, f satisfy (1.2). Fix $c_1 > 0$. Let $\mathcal{T}_{geo,\sigma}^{L,n}$ be a geometric boundary layer mesh in sense of Definition 2.3.*

Then there are constants C, b, $\beta > 0$ depending solely on the data A, c, f, Ω, on the parameter c_1, on the (fixed) macro-triangulation $\mathcal{T}^{\mathcal{M}}$, and on $\sigma \in (0,1)$ such that the following holds: If $\varepsilon \in (0,1]$ and L satisfy the scale resolution condition

$$\frac{\sigma^L}{\varepsilon} \le c_1, \tag{4.1}$$

then for every $q, n \in \mathbb{N}$ the solution $u_\varepsilon \in H_0^1(\Omega)$ of (1.1) can be approximated from $S_0^q(\Omega, \mathcal{T}_{geo,\sigma}^{L,n})$ such that

$$\inf_{v \in S_0^q(\Omega, \mathcal{T}_{geo,\sigma}^{L,n})} \|u_\varepsilon - v\|_{\varepsilon,\Omega} \le C q^9 \left[\varepsilon^\beta \sigma^{(1-\beta)n} + e^{-bq}\right], \tag{4.2}$$

$$N := \dim S_0^q(\Omega, \mathcal{T}_{geo,\sigma}^{L,n}) \le C\big(L^2 q^2 \operatorname{card} \mathcal{T}^{\mathcal{M}} + n q^2 J\big). \tag{4.3}$$

Proof. We employ the regularity theory for the solution u_ε presented in [18, Thms. 2.3.1, 2.3.4]. The infimum in (4.2) is realized with the aid of an interpolation operator Π_q defined elementwise by

$$(\Pi_q u)|_K \circ F_K := \begin{cases} \widehat{\Pi}_q^{\triangle}(u \circ F_K) & \text{if } K \text{ is a triangle} \\ \widehat{\Pi}_q^{\square}(u \circ F_K) & \text{if } K \text{ is a rectangle.} \end{cases}$$

Here, the operator $\widehat{\Pi}_q^{\triangle}$ is defined in Lemma 3.1 and the operator $\widehat{\Pi}_q^{\square}$ in Lemma 3.2. Note that since $\widehat{\Pi}_q^{\triangle}$ and $\widehat{\Pi}_q^{\square}$ reduce to the Gauss-Lobatto interpolation operator on the edges of the reference element, the operator Π_q indeed maps into $S_0^q(\Omega, \mathcal{T}_{geo,\sigma}^{L,n})$. We recall that the element maps F_K have the form

$$F_K = F_{K^{\mathcal{M}}} \circ A_K,$$

where $A_K : \widehat{K} \to \widetilde{K} := A_K(\widehat{K}) = F_{K^{\mathcal{M}}}^{-1}(K) \subset \widetilde{S}$ is an affine bijection. Indeed, for triangular elements it is clear that A_K is affine and for rectangular elements, this follows from the special form of the reference patches (cf. also Lemma 2.8, (i)).

The notation $\widehat{u}$ denotes the pull-back of u to the reference element, i.e., $\widehat{u} := u|_K \circ F_K$ whereas $\widetilde{u} := (u \circ F_{K^{\mathcal{M}}})|_{\widetilde{K}} = \widehat{u} \circ A_K^{-1}$ is the corresponding function on $\widetilde{K}$. We recall the notation $\widetilde{\Pi}_q$ from (3.6) and note that on a macro-element $K^{\mathcal{M}}$ we have

$$(\Pi_q u) \circ F_{K^{\mathcal{M}}} = \widetilde{\Pi}_q \widetilde{u}.$$

For $k \in \mathbb{N}_0$ we have for all elements $K \subset K^{\mathcal{M}}$ with $\widetilde{K} = F_{K^{\mathcal{M}}}^{-1}(K)$

$$\forall v \in H^k(K)\colon \quad \|v \circ F_{K^{\mathcal{M}}}\|_{H^k(\widetilde{K})} \sim \|v\|_{H^k(K)}, \tag{4.4a}$$

$$\forall v \in W^{k,\infty}(K)\colon \quad \|v \circ F_{K^{\mathcal{M}}}\|_{W^{k,\infty}(\widetilde{K})} \sim \|v\|_{W^{k,\infty}(K)}, \tag{4.4b}$$

where in both cases the constants implied in $\sim$ depend solely on k and the macro-element $K^{\mathcal{M}}$. The equivalences (4.4) show that the approximation error $v - \Pi_q v$ on K is equivalent to the corresponding error $\widetilde{v} - \widetilde{\Pi}_q \widetilde{v}$ on $\widetilde{K}$.

The approximation theory distinguishes between the "asymptotic case" $q\varepsilon \geq \kappa$ of large polynomial degree q and the "preasymptotic case" $q\varepsilon \leq \kappa$, where the parameter $\kappa > 0$ (depending only on A, c, f, Ω, the macro-triangulation, and σ) is of size $O(1)$ and will be determined in the course of the analysis of the "asymptotic case" in Step I.

Step I: Asymptotic case $q\varepsilon \geq \kappa$. We consider mesh patches $K^{\mathcal{M}}$ that abutt on a vertex $\boldsymbol{A}_j$ and those with a positive distance from the vertices separately in Steps I.1 and I.2.

Step I.1: $K^{\mathcal{M}}$ abutts on a vertex $\boldsymbol{A}_j$: The regularity of [18, Thm. 2.3.1] asserts the existence of C, $\gamma > 0$, $\beta_j \in [0,1)$ such that with $r_j(\cdot) := \operatorname{dist}(\cdot, \boldsymbol{A}_j)$, there holds for every $p \in \mathbb{N}_0$ and for every $0 < \varepsilon \leq 1$

$$|\nabla^p(u_\varepsilon(\cdot) - u_\epsilon(\boldsymbol{A}_j))| \leq C\gamma^p \varepsilon^{-1} \min\{1, r_j(\cdot)/\varepsilon\}^{1-\beta_j} (r_j(\cdot))^{-p} \max\{p+1, r_j(\cdot)/\varepsilon\}^{p+1}. \tag{4.5}$$

Recall from (3.5) that $\widetilde{r}(\cdot) = \operatorname{dist}(\cdot, \mathbf{0})$. Set $\widetilde{u}_\varepsilon := u_\varepsilon \circ F_{K^{\mathcal{M}}}$. Note $F_{K^{\mathcal{M}}}(\mathbf{0}) = \boldsymbol{A}_j$ and $\widetilde{r}(\widetilde{\mathbf{x}}) \sim r_j(F_{K^{\mathcal{M}}}(\widetilde{\mathbf{x}}))$. The analyticity of $F_{K^{\mathcal{M}}}$ and Lemma A.2 imply, for suitably modified constants C, γ independent of $\varepsilon \in (0,1]$, for every $p \in \mathbb{N}$

$$|\nabla^p(\widetilde{u}_\varepsilon(\cdot) - \widetilde{u}(\mathbf{0}))| \leq C\gamma^p \varepsilon^{-1} \min\{1, \widetilde{r}/\varepsilon\}^{1-\beta_j} (\widetilde{r}(\cdot))^{-p} \max\{p+1, \widetilde{r}(\cdot)/\varepsilon\}^{p+1} \quad \text{on } \widetilde{K}. \tag{4.6}$$

Lemma 3.3 then yields

$$\|\widetilde{u}_\varepsilon - \widetilde{\Pi}_q \widetilde{u}_\varepsilon\|_{L^\infty(K^{\mathcal{M}})} + \|\nabla(\widetilde{u}_\varepsilon - \widetilde{\Pi}_q \widetilde{u}_\varepsilon)\|_{L^\infty(K^{\mathcal{M}})} \leq Cq^9 \left(\sigma^{(1-\beta_j)n} + e^{-bq}\right)$$

provided that κ is a sufficiently large (depending on γ).

Step I.2: $K^{\mathcal{M}}$ does not abutt on a vertex $\boldsymbol{A}_j$: [18, Thm. 2.3.1] asserts

$$\forall \mathbf{x} \in K^{\mathcal{M}} \quad \forall p \in \mathbb{N}_0\colon \quad |\nabla^p u(\mathbf{x})| \leq C\gamma^p \max\{p+1, \varepsilon^{-1}\}^{p+2} \tag{4.7}$$

for constants C, $\gamma > 0$ independent of $\varepsilon \in (0,1]$. Since $K^{\mathcal{M}}$ is a trivial patch, it consists of a single (curvilinear) quadrilateral. The analyticity of $F_{K^{\mathcal{M}}} = F_K$ and Lemma A.2 imply, for suitably modified C, γ independent of $\varepsilon \in (0,1]$, that

$$\forall \widehat{\mathbf{x}} \in \widehat{S} \quad \forall p \in \mathbb{N}_0\colon \quad |\nabla^p \widehat{u}(\widehat{\mathbf{x}})| \leq C\gamma^p \max\{p+1, \varepsilon^{-1}\}^{p+2}\ . \tag{4.8}$$

Lemma 3.2 then implies that there are C, $b > 0$ such that for sufficiently large, fixed κ and for every $\varepsilon \in (0,1]$ and every $q \in \mathbb{N}$ holds

$$\|\widehat{u} - \widehat{\Pi}_q \widehat{u}\|_{L^\infty(K^{\mathcal{M}})} + \|\nabla(\widehat{u} - \widehat{\Pi}_q \widehat{u})\|_{L^\infty(\widehat{S})} \leq Ce^{-bq}\ .$$

Step I.3: Combining the approximation results of Steps I.1, I.2 for the finitely many patches leads to the desired estimate (4.2).

Step II: Preasymptotic case $q\varepsilon \leq \kappa$. The parameter κ has been fixed in Step I through the appeal to Lemmas 3.3 and 3.2. In the regime $q\varepsilon \leq \kappa$, we employ

the regularity theory of [18, Thm. 2.3.4], which furnishes the decomposition $u_\varepsilon = w_\varepsilon + \chi^{\mathsf{BL}} u_\varepsilon^{\mathsf{BL}} + \chi^{\mathsf{CL}} u_\varepsilon^{\mathsf{CL}} + r_\varepsilon$ into a smooth part w_ε, a boundary layer part $u_\varepsilon^{\mathsf{BL}}$, a corner layer part $u_\varepsilon^{\mathsf{CL}}$, and a small remainder r_ε; the functions χ^{BL}, χ^{CL} are suitable localizations near the boundary and the vertices of Ω. We approximate each of these four contributions in turn.

Step II.1: Approximation of w_ε. By [18, Thm. 2.3.4] the smooth part w_ε is analytic on $\overline{\Omega}$ with constants independent of ε. Therefore, one can show $\|w_\varepsilon - \Pi_q w_\varepsilon\|_{W^{1,\infty}(\Omega)} \le Ce^{-bq}$ using similar techniques as in the asymptotic case above (essentially, setting $\varepsilon = 1$ there and ignoring the special treatment of the elements abutting on the vertices of Ω).

Step II.2: Approximation of $\chi^{\mathsf{BL}} u_\varepsilon^{\mathsf{BL}}$.

Step II.2.a: Regularity of $u_\varepsilon^{\mathsf{BL}}$: The regularity of $u_\varepsilon^{\mathsf{BL}}$ in [18, Thm. 2.3.4] is described in terms of boundary fitted coordinates (cf. Fig. 4.1). Associated with each edge Γ_j are fitted coordinates (ρ_j, θ_j), where ρ_j is the distance from the analytic continuation $\widetilde{\Gamma}_j$ of the boundary arc Γ_j, and θ_j is a parametrization of Γ_j. The map $\psi_j : (\rho_j, \theta_j) \mapsto (x, y) \in \Omega$ is analytic with an analytic inverse. An analytic arc Γ_j' emanates from each vertex $\boldsymbol{A}_j$, which can be chosen arbitrarily but is assumed to be such that the angles between Γ_j and Γ_j' and between Γ_{j+1} and Γ_j' are both less than π. Condition 8 of Definition 2.3 ensures that Γ_j' can be chosen to be a meshline of a boundary layer mesh since it can be chosen as the image of an edge of $\widetilde{S}$ or a diagonal of $\widetilde{S}$ under a patch map.

The regions $\Omega_j \subset \{\mathbf{x} \in \Omega \,|\, \operatorname{dist}(\mathbf{x}, \Gamma_j) < \delta\}$ for a sufficiently small δ are confined by the lines Γ_j, Γ_j', and Γ_{j-1}' as shown in Fig. 4.2. By [18, Thm. 2.3.4], the function $u_\varepsilon^{\mathsf{BL}}$ is analytic on each Ω_j and satisfies there, for constants C, γ, $\alpha > 0$ independent of $\varepsilon \in (0, 1]$ and all $(m, n) \in \mathbb{N}_0$,

$$
\begin{aligned}
|\partial_{\rho_j}^n \partial_{\theta_j}^m u_\varepsilon^{\mathsf{BL}} \circ \psi_j(\rho_j, \theta_j)| &\overset{[18,\ \text{Thm. 2.3.4}]}{\le} C\varepsilon^{-n}\gamma^{n+m} m! e^{-\alpha\rho_j/\varepsilon} \\
&\le C\gamma^{n+m} \max\{n+m, \varepsilon^{-1}\}^{n+m} e^{-\alpha\rho_j/\varepsilon} \,. \qquad (4.9)
\end{aligned}
$$

Finally, the cut-off function χ^{BL} is supported by $\cup_j \overline{\Omega_j}$ and is identically 1 near $\partial\Omega$.

Step II.2.b: Approximation of $\chi^{\mathsf{BL}} u_\varepsilon^{\mathsf{BL}}$ far from $\partial\Omega$: In the interest of simplicity of notation, we make the assumption that patches $K^{\mathcal{M}}$ touching $\partial\Omega$ are fully contained in the tubular neighborhood $\cup_j \overline{\Omega_j}$ of $\partial\Omega$. Since patches $K^{\mathcal{M}}$ not touching $\partial\Omega$ have a positive distance from $\partial\Omega$, the function $\chi^{\mathsf{BL}} u_\varepsilon^{\mathsf{BL}}$ is exponentially small (in $1/\varepsilon$) there; in view of the stability (3.7) (and thus the stability of Π_q) $\|\chi^{\mathsf{BL}} u_\varepsilon^{\mathsf{BL}} - \Pi_p(\chi^{\mathsf{BL}} u_\varepsilon^{\mathsf{BL}})\|_{W^{1,\infty}(K)} \le Ce^{-b/\varepsilon}$ for $K \in K^{\mathcal{M}}$. Since $q/\kappa \le 1/\varepsilon$ the error contribution of these patches is controlled in the desired fashion.

Step II.2.c: Approximation of $\chi^{\mathsf{BL}} u_\varepsilon^{\mathsf{BL}}$ near $\partial\Omega$: Let $K^{\mathcal{M}}$ be a patch touching $\partial\Omega$. Consider, for a fixed j the pull-back $F_{K^{\mathcal{M}}}^{-1}(K^{\mathcal{M}} \cap \Omega_j)$. By the assumptions of the boundary layer mesh (Def. 2.3) this pull back is either empty, the full square $\widetilde{S}$, half the square $\widetilde{T} = \{\widetilde{\mathbf{x}} = (\widetilde{x}, \widetilde{y}) \,|\, 0 < \widetilde{x} < 1, 0 < \widetilde{y} < \widetilde{x}\}$, or the other half $\widetilde{T}^{\text{flip}} = \{\widetilde{\mathbf{x}} = (\widetilde{x}, \widetilde{y}) \,|\, 0 < \widetilde{x} < 1, \widetilde{x} < \widetilde{y} < 1\}$.

To fix ideas, let us assume that $K^{\mathcal{M}}$ is a mixed patch. The reference mixed patch restricted to $\widetilde{T}$ is the half-patch $\widetilde{\mathcal{T}}^{\mathsf{M},\text{half},L,n}$ and its restriction to $\widetilde{T}^{\text{flip}}$ is $\widetilde{\mathcal{T}}^{\mathsf{C},\text{half},\text{flip},n}$. We approximate $(\chi^{\mathsf{BL}} u_\varepsilon^{\mathsf{BL}}) \circ F_{K^{\mathcal{M}}}$ on these two parts separately, starting with the approximation on $\widetilde{T}$. The assumptions on boundary layer meshes (Def. 2.3) allow us to assume that $F_{K^{\mathcal{M}}}(\widetilde{T}) \subset \Omega_j$ for some j. We recall that $F_{K^{\mathcal{M}}}$ maps the edge $\{\widetilde{y} = 0\}$ of $\widetilde{T}$ to (a subset of) $\partial\Omega$, which corresponds to $\rho_j = 0$ in the boundary fitted

coordinates. The shape-regularity of $F_{K^{\mathcal{M}}}$ implies that $\psi_j^{-1} \circ F_{K^{\mathcal{M}}}$ has the form

$$\widetilde{T} \ni (\widetilde{x}, \widetilde{y}) \mapsto (\rho_j, \theta_j) = (\widetilde{y}\rho(\widetilde{x}, \widetilde{y}), \theta(\widetilde{x}, \widetilde{y})) \tag{4.10}$$

for a pair of functions ρ, θ with $\rho \geq \rho_0 > 0$. The analyticity of ψ_j^{-1} and $F_{K^{\mathcal{M}}}$ implies that ρ and θ are in fact analytic on $\overline{\widetilde{T}}$. Hence, the transformed function

$$\widetilde{u}_\varepsilon^{\mathsf{BL}} := u_\varepsilon^{\mathsf{BL}} \circ F_{K^{\mathcal{M}}} = u_\varepsilon^{\mathsf{BL}} \circ \psi_j \circ (\psi_j^{-1} \circ F_{K^{\mathcal{M}}}) \tag{4.11}$$

admits by Lemma A.1 and (4.9) the analytic regularity

$$\forall (m,n) \in \mathbb{N}_0^2 \quad \forall (\widetilde{x}, \widetilde{y}) \in \widetilde{T}\colon \quad |\partial_{\widetilde{x}}^m \partial_{\widetilde{y}}^n \widetilde{u}_\varepsilon^{\mathsf{BL}}(\widetilde{x}, \widetilde{y})| \leq C\gamma^{m+n} m! \max\{n+1, \varepsilon^{-1}\}^n e^{-b\widetilde{y}/\varepsilon}, \tag{4.12}$$

where the constants C, γ, $b > 0$ are independent of $\varepsilon \in (0,1]$. We decompose the set of elements $\widetilde{\mathcal{T}}^{\mathsf{M},\mathrm{half},L,n}$ into two sets $\widetilde{\mathcal{T}}_1 := \{\widetilde{K} \in \widetilde{\mathcal{T}}_{geo,\sigma}^{\mathsf{M},\mathrm{half},L,n} \,|\, \widetilde{\chi}^{\mathsf{BL}}|_{\widetilde{K}} \equiv 1\}$ and $\widetilde{\mathcal{T}}_2 := \widetilde{\mathcal{T}}_{geo,\sigma}^{\mathsf{M},\mathrm{half},L,n} \setminus \widetilde{\mathcal{T}}_1$. For the elements of $\widetilde{\mathcal{T}}_1$, Lemma 3.4, (i) and (4.12) give that there are C, $b > 0$ such that for every $q \in \mathbb{N}$ and every $\widetilde{K} \in \widetilde{\mathcal{T}}_1$

$$\|\widetilde{\chi}^{\mathsf{BL}}\widetilde{u}_\varepsilon^{\mathsf{BL}} - \widetilde{\Pi}_q(\widetilde{\chi}^{\mathsf{BL}}\widetilde{u}_\varepsilon^{\mathsf{BL}})\|_{L^\infty(\widetilde{K})} + \varepsilon\|\widetilde{\chi}^{\mathsf{BL}}\widetilde{u}_\varepsilon^{\mathsf{BL}} - \widetilde{\Pi}_q(\widetilde{\chi}^{\mathsf{BL}}\widetilde{u}_\varepsilon^{\mathsf{BL}})\|_{L^\infty(\widetilde{K})} \leq Ce^{-bq}. \tag{4.13}$$

For the elements of the set $\widetilde{\mathcal{T}}_2$, we use (4.10) to see that $\widetilde{K} \in \widetilde{\mathcal{T}}_2$ implies $\mathrm{dist}(\widetilde{K}, \{\widetilde{y} = 0\}) > c$ for some $c > 0$ that depends solely on $F_{K^{\mathcal{M}}}$ and ψ_j. Hence, the smoothness of $\widetilde{\chi}^{\mathsf{BL}}$ and (4.12) provide $\|\widetilde{\chi}^{\mathsf{BL}}\widetilde{u}_\varepsilon^{\mathsf{BL}}\|_{W^{1,\infty}(\widetilde{K})} \leq Ce^{-b/\varepsilon}$ for suitable C, $b > 0$ and every $\widetilde{K} \in \widetilde{\mathcal{T}}_2$. Hence, the stability properties of $\widetilde{\Pi}_q$ provided in (3.7) and $q/\kappa \leq 1/\varepsilon$ imply for all $\widetilde{K} \in \widetilde{\mathcal{T}}_2$

$$\|\widetilde{\chi}^{\mathsf{BL}}\widetilde{u}_\varepsilon^{\mathsf{BL}} - \widetilde{\Pi}_q(\widetilde{\chi}^{\mathsf{BL}}\widetilde{u}_\varepsilon^{\mathsf{BL}})\|_{L^\infty(\widetilde{K})} + \varepsilon\|\widetilde{\chi}^{\mathsf{BL}}\widetilde{u}_\varepsilon^{\mathsf{BL}} - \widetilde{\Pi}_q(\widetilde{\chi}^{\mathsf{BL}}\widetilde{u}_\varepsilon^{\mathsf{BL}})\|_{L^\infty(\widetilde{K})} \leq Ce^{-bq}. \tag{4.14}$$

Let us now sketch the arguments for the approximation of $\widetilde{\chi}^{\mathsf{BL}}\widetilde{u}_\varepsilon^{\mathsf{BL}}$ on $\widetilde{T}^{\mathrm{flip}}$. For notational simplicity, assume that $F_{K^{\mathcal{M}}}(\widetilde{T}^{\mathrm{flip}}) \subset \Omega_j$. (If $F_{K^{\mathcal{M}}}(\widetilde{T}^{\mathrm{flip}}) \subset \Omega_{j'}$ for some different j', then replace j with j' in what follows.) The regularity assertion (4.12) is still valid. Next, one observes that on $\widetilde{T}^{\mathrm{flip}}$, one has $\widetilde{y} \sim \widetilde{r}(\widetilde{x}, \widetilde{y}) = \mathrm{dist}((\widetilde{x}, \widetilde{y}), \mathbf{0})$. Hence, recalling (4.12), $\widetilde{u}_\varepsilon^{\mathsf{BL}}$ even satisfies, for suitable C, $b > 0$ and all $p \in \mathbb{N}_0$,

$$|\nabla^p \widetilde{u}_\varepsilon^{\mathsf{BL}}| \leq C \max\{p+1, \varepsilon^{-1}\}^p e^{-b\widetilde{r}(\cdot)/\varepsilon} \quad \text{on } \widetilde{T}^{\mathrm{flip}}. \tag{4.15}$$

Replacing the appeal to Lemma 3.4, (i) with that to Lemma 3.4, (ii), we may argue as above to obtain

$$\|\widetilde{\chi}^{\mathsf{BL}}\widetilde{u}_\varepsilon^{\mathsf{BL}} - \widetilde{\Pi}_q\widetilde{\chi}^{\mathsf{BL}}\widetilde{u}_\varepsilon^{\mathsf{BL}}\|_{L^\infty(\widetilde{T}^{\mathrm{flip}})} + \varepsilon\|\nabla(\widetilde{\chi}^{\mathsf{BL}}\widetilde{u}_\varepsilon^{\mathsf{BL}} - \widetilde{\Pi}_q\widetilde{\chi}^{\mathsf{BL}}\widetilde{u}_\varepsilon^{\mathsf{BL}})\|_{L^\infty(\widetilde{T}^{\mathrm{flip}})} \leq Ce^{-bq}.$$

This concludes the arguments for the approximation of $\widetilde{u}_\varepsilon^{\mathsf{BL}}$ on a mixed patch $\widetilde{\mathcal{T}}_{geo,\sigma}^{\mathsf{M},L,n}$. The approximation on corner patches $\widetilde{\mathcal{T}}_{geo,\sigma}^{\mathsf{C},n}$, tensor patches $\widetilde{\mathcal{T}}_{geo,\sigma}^{\mathsf{T},n}$, or boundary layer patches $\widetilde{\mathcal{T}}_{geo,\sigma}^{\mathsf{BL},L}$ is similar.

Step II.3: Approximation of $\chi^{\mathsf{CL}}u_\varepsilon^{\mathsf{CL}}$: Structurally, the proof is similar to the procedure in Step II.2. From [18, Thm. 2.3.4] we have in a neighborhood B_j of vertex $\boldsymbol{A}_j$ that $u_\varepsilon^{\mathsf{CL}}$ satisfies on $(B_j \cap \Omega_j) \cup (B_j \cap \Omega_{j+1})$ with $r_j = \mathrm{dist}(\cdot, A_j)$

$$\forall p \in \mathbb{N}_0\colon \quad |\nabla^p u_\varepsilon^{\mathsf{CL}}| \leq C\gamma^p p! \varepsilon^{\beta_j - 1}(r_j(\cdot))^{1-p-\beta_j} e^{-\alpha r_j(\cdot)/\varepsilon}, \tag{4.16}$$

where C, $\alpha > 0$ and $\beta_j \in [0,1)$ are independent of $\varepsilon \in (0,1]$. Let $K^{\mathcal{M}}$ be a patch abutting on $\boldsymbol{A}_j$. Such a patch has to be either a corner patch or a mixed patch. Then $K^{\mathcal{M}} \cap \Omega_j$ (and similarly $K^{\mathcal{M}} \cap \Omega_{j+1}$) consists of one or two half-patches that are push-forwards of $\widetilde{\mathcal{T}}' \in \{\widetilde{\mathcal{T}}^{\mathsf{M},\mathrm{half},L,n}_{geo,\sigma}, \widetilde{\mathcal{T}}^{\mathsf{C},\mathrm{half},n}_{geo,\sigma}, \widetilde{\mathcal{T}}^{\mathsf{C},\mathrm{half,flip},n}_{geo,\sigma}\}$. For simplicity of exposition, assume that $K^{\mathcal{M}} \subset B_j$. By the analyticity of $F_{K^{\mathcal{M}}}$, the shape regularity of $F_{K^{\mathcal{M}}}$ together with $F_{K^{\mathcal{M}}}(\mathbf{0}) = \boldsymbol{A}_j$, and Lemma A.2 we get that $\widetilde{u}^{\mathsf{CL}}_\varepsilon := u^{\mathsf{CL}}_\varepsilon \circ F_{K^{\mathcal{M}}}$ satisfies on $\mathcal{O} := F^{-1}_{K^{\mathcal{M}}}(K^{\mathcal{M}} \cap \Omega_j)$

$$\forall p \in \mathbb{N}_0\colon \quad |\nabla^p \widetilde{u}^{\mathsf{CL}}_\varepsilon| \le C\gamma^p p! \varepsilon^{\beta_j - 1} (\widetilde{r}(\cdot))^{1-p-\beta_j} e^{-\alpha \widetilde{r}(\cdot)/\varepsilon}; \tag{4.17}$$

here, we suitably adjusted C, γ, $\alpha > 0$. We also note that the pull-back $\widetilde{\chi}^{\mathsf{CL}}$ is smooth and identically 1 near $\mathbf{0}$. Hence, using Lemma 3.5 we obtain

$$\begin{aligned} &\|\widetilde{\chi}^{\mathsf{CL}} \widetilde{u}^{\mathsf{CL}}_\varepsilon - \widetilde{\Pi}_q(\widetilde{\chi}^{\mathsf{CL}} \widetilde{u}^{\mathsf{CL}}_\varepsilon)\|_{L^2(\mathcal{O})} + \varepsilon \|\nabla(\widetilde{\chi}^{\mathsf{CL}} \widetilde{u}^{\mathsf{CL}}_\varepsilon - \widetilde{\Pi}_q(\widetilde{\chi}^{\mathsf{CL}} \widetilde{u}^{\mathsf{CL}}_\varepsilon)\|_{L^2(\mathcal{O})} \\ &\qquad \le C\left(\varepsilon e^{-bq} + \varepsilon^{\beta_j} q^4 \sigma^{n(1-\beta_j)}\right). \end{aligned}$$

Step II.4: Approximation of r_ε: We approximate r_ε by zero. We note that [18, Thm. 2.3.4] asserts that $r_\varepsilon|_{\partial\Omega} = 0$ and that $\|r_\varepsilon\|_{H^1(\Omega)} \le Ce^{-b/\varepsilon}$ for suitable C, $b > 0$ independent of $\varepsilon \in (0,1]$. ∎

Theorem 4.1 restricted to $\varepsilon \in (0,1]$. For $\varepsilon \ge 1$, (1.1) is regularly perturbed and exponential convergence is afforded by standard *hp*-approximation results [18, 29]. For completeness, we state

Proposition 4.2. *Assume the hypotheses on Ω and the data A, c, f as in Theorem 4.1. Let $\mathcal{T}^{L,n}_{geo,\sigma}$ be a geometric boundary layer mesh. Then, there are constants C, $b > 0$, $\beta \in [0,1)$ depending solely on A, c, f, the analyticity properties of the patch maps for the macro-triangulation, and σ such that for any $\varepsilon \ge 1$, the solution u_ε of (1.1) satisfies for every n, L, $q \in \mathbb{N}$*

$$\inf_{v \in S^q_0(\Omega, \mathcal{T}^{L,n}_{geo,\sigma})} \|u_\varepsilon - v\|_{H^1(\Omega)} \le C\varepsilon^{-2}\left(q^9 \sigma^{(1-\beta)n} + e^{-bq}\right). \tag{4.18}$$

Proof. The solution $u_\varepsilon \in H^1_0(\Omega)$ satisfies

$$-\nabla \cdot (A\nabla u_\varepsilon) + \varepsilon^{-2} c u_\varepsilon = \varepsilon^{-2} f \quad \text{in } H^{-1}(\Omega). \tag{4.19}$$

For $\varepsilon \ge 1$, the term $\varepsilon^{-2}c$ represents a regular perturbation and the analytic regularity theory for linear, second order elliptic boundary value problems (e.g. [5] and the references there) is applicable. The resulting regularity assertions are then those employed in the "asymptotic case" in the proof of Theorem 4.1 with $\varepsilon = 1$ there. The factor ε^{-2} in (4.18) is a reflection of the fact that the right-hand side of (4.19) include the factor ε^{-2}. ∎

5. Numerical experiments. For $0 < \varepsilon \le 1$ and $f \equiv 1$ we consider the Dirichlet problem: find $u_\varepsilon \in H^1_0(\Omega)$ such that

$$-\varepsilon^2 \Delta u_\varepsilon + u_\varepsilon = f \quad \text{in} \quad H^{-1}(\Omega).$$

Here, the domain Ω is either the unit square $\Omega_1 = (0,1)^2$, the so-called "L-shaped, polygonal domain" $\Omega_2 \subset \mathbb{R}^2$ determined by the vertices $\{(0,0),(1,0),(1,1),(-1,1),(-1,-1),(0,-1)\}$, or the square domain with a slit $\Omega_3 = (-1,1)^2 \setminus (-1,0] \times \{0\}$.

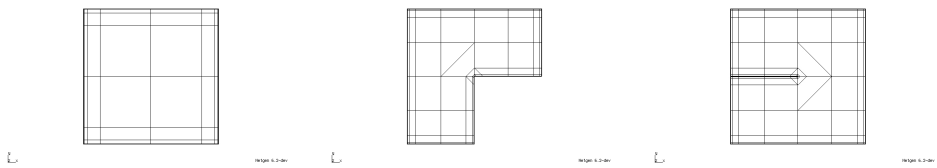

FIG. 5.1. *Examples of geometric boundary layer meshes for the three domains* $\Omega = \Omega_j$, $j = 1, 2, 3$, *ordered from left to right (cf. Sec. 5).*

In Figure 5.1 we show examples of the meshes used for the three domains. These are constructed using the NGSolve/Netgen package [24]. For the square domain $\Omega = \Omega_1$ the resulting mesh is the geometric boundary layer mesh $\mathcal{T}^{L,L}_{geo,\sigma}$ with $L = 4$ and $\sigma = 0.25$. The same parameters are used in NGSolve/Netgen to construct the meshes for the other two domains, with the resulting meshes differing slightly from the strict definition of $\mathcal{T}^{L,L}_{geo,\sigma}$ near the re-entrant corners. Nevertheless, we denote these meshes also by $\mathcal{T}^{L,L}_{geo,\sigma}$ and make use of the finite element spaces $S^q_0(\Omega, \mathcal{T}^{L,L}_{geo,\sigma})$.

For each $p = 1, 2, 3, \ldots$, we use the finite element space $S^q_0(\Omega, \mathcal{T}^{L,L}_{geo,\sigma})$ with uniform polynomial order $q = p$ and with $L = p$ refinement levels towards boundaries and corners with refinement factor $\sigma = 0.25$. We denote by $u^h_\varepsilon \in S^p_0(\Omega, \mathcal{T}^{p,p}_{geo,\sigma})$ the corresponding finite element solution. We measure the error in energy norm

$$\text{error} = \left(\varepsilon^2 \|\nabla(u_\varepsilon - u^h_\varepsilon)\|^2_{L^2(\Omega)} + \|u_\varepsilon - u^h_\varepsilon\|^2_{L^2(\Omega)}\right)^{1/2}, \tag{5.1}$$

where u^h_ε denotes the discrete solution. In place of the (unknown, for the considered examples) exact solution u_ε we use a numerical approximation on a sufficiently fine mesh. The plots of the estimated numerical errors for the three domains are depicted in Figures 5.2–5.4. Evidently, exponential convergence occurs. In agreement with the theoretical analysis, the experimentally observed exponential convergence has two regimes: (i) an asymptotic regime in which the scale resolution condition $\sigma^p \lesssim \varepsilon$ is satisfied and (ii) a pre-asymptotic regime with $\sigma^p \gtrsim \varepsilon$. The observed exponential convergence in the preasymptotic regime (not rigorously shown in Theorem 4.1) is plausible for the following reason: the approximation error for boundary layer functions is dominated by the error on the elements touching the boundary and is of size $O(\sigma^{p/2})$ for every $p \in \mathbb{N}$. The approximation error of the corner layer functions is likewise dominated by the error on the elements abutting on the vertices of Ω and is of size $O(\sigma^{p(1-\beta)})$ for every $p \in \mathbb{N}$ and some fixed $\beta \in [0, 1)$.

6. Conclusions. We established robust exponential convergence of *hp*-FEM for solutions of elliptic singular perturbation problems in polygons. These solutions contain, usually, boundary layers, corner singularities and combinations of the two. We admitted possibly multiple length scales, and built the *hp*-FE approximations on (patches of) geometric boundary layer meshes as described in Section 2, and depicted in Fig. 2.1. The *hp*-FEM on this class of partitions is capable to resolve exponential boundary- and corner-layers with multiple physical length scales under a scale resolution condition that incorporates the smallest physical length scale. The number of geometric mesh refinements to achieve this grows only logarithmically with respect to the smallest length scale.

As we explained in the numerical experiments section meshes of this type are generated, in general geometries, by specialized mesh generators such as NETGEN

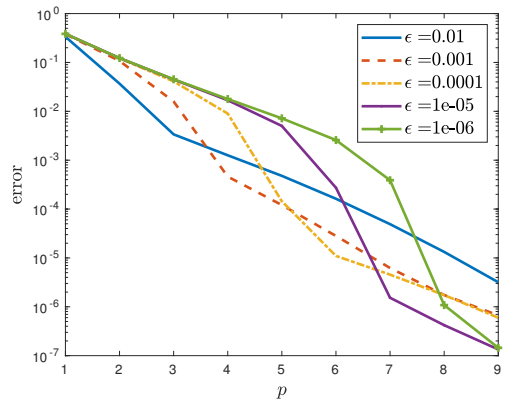

Fig. 5.2. *Convergence in the energy norm (5.1) for the square domain for different values of ε and $q = L = n = p$.*

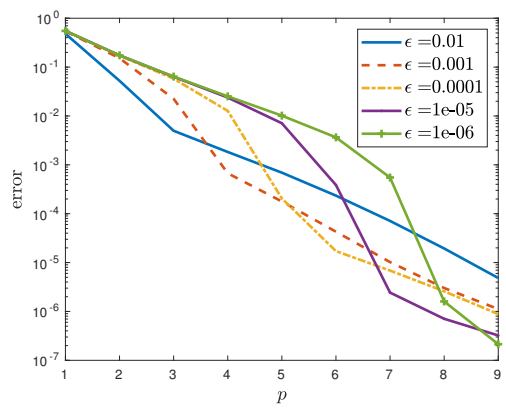

Fig. 5.3. *Convergence in the energy norm (5.1) for the L-shaped domain for different values of ε and $q = L = n = p$.*

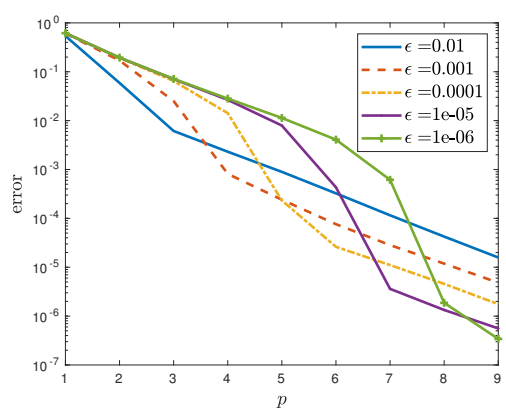

Fig. 5.4. *Convergence in the energy norm (5.1) for the slit domain for different values of ε and $q = L = n = p$.*

[24]. We hasten to add, however, that our analysis can readily be extended to cover more general partitions, such as geometric boundary layer meshes that also contain anisotropic triangles.

The focus of the present work was on robust exponential convergence rate bounds for singular perturbation problems in nonsmooth domains by *hp* finite element methods. We proved that they afford robust, exponential convergence on patchwise structured meshes with possibly anisotropic, geometric refinement towards the "support set" (i.e., the subset of $\overline{\Omega}$ off which the layer components decay exponentially), of the boundary and corner layers. As a rule, robust exponential convergence requires genuine *hp*-FE capabilities, i.e. simultaneous mesh refinement and polynomial degree increase, as featured in the *hp*-FE spaces $\{S_0^p(\Omega, \mathcal{T}_{geo,\sigma}^{p,p})\}_{p\geq 1}$ used in our numerical experiments. The corresponding, patchwise structured triangulations can be automatically generated by specialized mesh generators, in domains of engineering interest (see, e.g., [24]). Although we mainly considered the model linear, second order elliptic singular perturbation problem (1.1), corresponding solution families are known to arise for several common models in solid and fluid mechanics, see, e.g. [2,9,12,13] and the references there.

The underlying concept of using patchwise structured meshes to approximate parametric solution families to linear, elliptic singularly perturbed boundary value problems extends also to *h*-version FEM. Here, in patches abutting on the boundary analogs of so-called "Shishkin meshes", see, e.g., [32], [23, Sec. 3.5.2], could be employed to achieve robust, algebraic rates of convergence under weaker, finite order differentiability assumptions on the data A, c, and f than the presently assumed analyticity in $\overline{\Omega}$ of these data.

The model problem (1.1) considers homogeneous Dirichlet boundary conditions. The approximation result Theorem 4.1 relies on the regularity results of [18], which decomposes the solution (1.1) into boundary and corner layer components. Similar decompositions can be expected to hold also for other boundary conditions. Then the approximation results of Section 3 are applicable indicating that *hp*-FEM on similarly patchwise structured meshes will likewise lead to robust exponential convergence.

Appendix A. Analytic changes of variables. The following lemma shows how boundary layer functions are transformed under the patch maps if the edge $\{\widetilde{y} = 0\}$ of $\widetilde{S}$ is mapped to a subset of $\partial\Omega$:

LEMMA A.1. *Let $G_x \subset \mathbb{R} \times \mathbb{R}^+$ be a domain. Let the map $M : (\widetilde{x}, \widetilde{y}) \mapsto (\theta, \rho)$ be of the form $M(\widetilde{x}, \widetilde{y}) = (\check{\theta}(\widetilde{x}, \widetilde{y}), y\check{\rho}(x, y))$ for some functions $\check{\theta}$, $\check{\rho} \geq \rho_0 > 0$ that are analytic on* closure(G_x)*, i.e., there are constants $C_M, \gamma_M > 0$ such that $\|\nabla^n \check{\theta}\|_{L^\infty(G_x)}$, $\|\nabla^n \check{\rho}\|_{L^\infty(G_x)} \leq C_M \gamma_M^n n!$ for all $n \in \mathbb{N}_0$. Let $\mathcal{O}_x \subset G_x$ be open and let $\mathcal{O}$ be an open neighborhood of $M(\mathcal{O}_x)$. Let u be analytic on $\mathcal{O}$ and assume that, for some function C_u and some constants $b > 0$, $\gamma > 0$, there holds*

$$\forall (m, n) \in \mathbb{N}_0^2 \quad \forall (\rho, \theta) \in \mathcal{O}: \quad |\partial_\rho^n \partial_\theta^m u(\theta, \rho)| \leq C_u(\theta, \rho) e^{-b\rho/\varepsilon} \gamma^{n+m} m! \max\{n, \varepsilon^{-1}\}^n.$$

Then there are constants b', $\widetilde{\gamma} > 0$ (depending only on b, γ, and M) such that the function $\widetilde{u} := u \circ M$ satisfies with the notation $(\rho, \theta) = M(\widetilde{x}, \widetilde{y})$

$$\forall (m, n) \in \mathbb{N}_0^2 \quad \forall (\widetilde{x}, \widetilde{y}) \in \mathcal{O}_x: \quad |\partial_{\widetilde{y}}^n \partial_{\widetilde{x}}^m \widetilde{u}(\widetilde{x}, \widetilde{y})| \leq C_u(\theta, \rho) e^{-b'\widetilde{y}/\varepsilon} \gamma^{n+m} m! \max\{n, \varepsilon^{-1}\}^n.$$

Proof. The proof uses arguments employed in [18, Sec. 4.3]. Consider a fixed $(\widetilde{x}, \widetilde{y}) \in \mathcal{O}_x$ and set $(\theta', \rho') = M(\widetilde{x}, \widetilde{y})$. Then $(\theta, \rho) \mapsto u(\theta, \rho)$ is holomorphic on the

polydisc

$$B_{1/\gamma}(\theta') \times B_{1/(\gamma e)}(\rho') \subset \mathbb{C}^2$$

with the bound

$$|u(\theta' + \zeta_1, \rho' + \zeta_2)| \le C_u(\rho', \theta') e^{-b\rho'/\varepsilon} \frac{1}{1 - \gamma|\zeta_1|} \left[\frac{1}{1 - \gamma e|\zeta_2|} + \exp\left(\gamma|\zeta_2|/\varepsilon\right) \right]. \tag{A.1}$$

Since the functions $\check\theta$, $\check\rho$ are holomorphic on the closure of $M(G_x)$, there are C_1, $\delta > 0$ (independent of $(\widetilde{x}, \widetilde{y}) \in G$) such that for ζ_1, $\zeta_2 \in B_\delta(0) \subset \mathbb{C}$ there holds

$$\begin{aligned} \left|\check\theta(\widetilde{x} + \zeta_1, y + \zeta_2) - \check\theta(\widetilde{x}, \widetilde{y})\right| &\le C_1 \left[|\zeta_1| + |\zeta_2|\right], \\ |(\widetilde{y} + \zeta_2)\check\rho(\widetilde{x} + \zeta_1, \widetilde{y} + \zeta_2) - \widetilde{y}\check\rho(\widetilde{x}, \widetilde{y})| &\le C_1 \left[y(|\zeta_1| + |\zeta_2|) + |\zeta_2|\right], \end{aligned}$$

and we may assume that $\delta > 0$ is such that for ζ_1, $\zeta_2 \in B_\delta(0)$ we have $M(\widetilde{x} + \zeta_1, \widetilde{y} + \zeta_2) \in B_{1/(2\gamma)}(\theta') \times B_{1/(2\gamma e)}(\rho')$. This implies in view of (A.1) the bounds

$$|\widetilde{u}(\widetilde{x} + \zeta_1, \widetilde{y} + \zeta_2)| = |u(M(\widetilde{x} + \zeta_1, \widetilde{y} + \zeta_2))| \tag{A.2}$$

$$\le C C_u(\theta', \rho') e^{-b\rho'/\varepsilon} \exp(C_1\gamma|\zeta_2|/\varepsilon) \exp\bigl(C_1\gamma\widetilde{y}\left[|\zeta_1| + |\zeta_2|\right]/\varepsilon\bigr). \tag{A.3}$$

For δ_1, $\delta_2 < \delta$ Cauchy's integral formula for derivatives gives

$$\partial_{\widetilde{x}}^{\alpha_1} \partial_{\widetilde{y}}^{\alpha_2} \widetilde{u}(\widetilde{x}, \widetilde{y}) = -\frac{\alpha_1! \alpha_2!}{4\pi^2} \int_{\zeta_1 \in \partial B_{\delta_1}(0)} \int_{\zeta_2 \in \partial B_{\delta_2}(0)} \frac{\widetilde{u}(x + \zeta_1, y + \zeta_2)}{(-\zeta_1)^{\alpha_1+1}(-\zeta_2)^{\alpha_2+1}} \, d\zeta_1 d\zeta_2$$

so that

$$\left|\partial_{\widetilde{x}}^{\alpha_1} \partial_{\widetilde{y}}^{\alpha_2} \widetilde{u}(\widetilde{x}, \widetilde{y})\right| \le C C_u(\rho', \theta') e^{-b\rho'/\varepsilon} \frac{\alpha_1!}{\delta_1^{\alpha_1}} \frac{\alpha_2!}{\delta_2^{\alpha_2}} \exp(C_1\gamma\delta_2/\varepsilon) \exp(C_1\gamma y(\delta_1 + \delta_2)/\varepsilon)$$

Selecting $\delta_1 = \delta := b\rho_0/(4C_1)$ and $\delta_2 = \min\{(|\alpha_2| + 1)\varepsilon, \delta\}$ yields the desired result with $b' = b/2$ since $C_1\widetilde{y}(\delta_1 + \delta_2)/\varepsilon \le 2\delta C_1\widetilde{y}/\varepsilon \le 2\delta C_1\rho'/\rho_0 = b/2$. ∎

The following lemma shows how functions that may have a singular behavior are transformed under analytic changes of variables:

Lemma A.2 ([18, Lemma 4.3.3]). *Let $\widetilde{G} \subset \mathbb{R}^2$ be a domain and $M : \widetilde{G} \to \mathbb{R}^2$ be analytic on* closure$(\widetilde{G})$. *Let $\widetilde{\mathcal{O}} \subset \widetilde{G}$ be open and $\mathcal{O}$ be an open neighborhood of $M(\widetilde{\mathcal{O}})$. Let u be analytic on $\mathcal{O}$ and assume that for some (positive) function Λ, $r : \mathcal{O} \to \mathbb{R}$ and some $\gamma \ge 0$ there holds*

$$\forall n \in \mathbb{N}_0 \quad \forall \mathbf{x} \in \mathcal{O}\colon \quad |\nabla^n u(\mathbf{x})| \le \Lambda(\mathbf{x})\gamma^n \max\{(n+1)/r(\mathbf{x}), \varepsilon^{-1}\}^n. \tag{A.4}$$

Then the function $\widetilde{u} := u \circ M$ is analytic on $\widetilde{\mathcal{O}}$ and there are constants C, $\widetilde{\gamma} > 0$ depending solely on M and γ such that for each $\widetilde{\mathbf{x}} \in \widetilde{\mathcal{O}}$ there holds with the notation $\mathbf{x} = M(\widetilde{\mathbf{x}})$

$$\forall n \in \mathbb{N}_0\colon \quad |\nabla^n \widetilde{u}(\widetilde{\mathbf{x}})| \le C\Lambda(\mathbf{x})\widetilde{\gamma}^n \max\{(n+1)/r(\mathbf{x}), \varepsilon^{-1}\}^n.$$

Proof. The statement is taken from [18, Lemma 4.3.3] except that we explicitly allow r to be a function of $\mathbf{x}$. The proof is similar to that of Lemma A.1. We fix $\widetilde{\mathbf{x}} \in \widetilde{G}$ and set $\mathbf{x} = M(\widetilde{\mathbf{x}})$. The assumption (A.4) implies that u has a holomorphic

extension to $B_{cr(\mathbf{x})}(\mathbf{x}) \subset \mathbb{C}^2$ with $c > 0$ depending solely on γ. Additionally, we have the bound for $z \in B_{cr(\mathbf{x})}(\mathbf{x}) \subset \mathbb{C}^2$ (we write $r = r(\mathbf{x})$)

$$|u(\mathbf{x}+z)| \le \Lambda(\mathbf{x}) \sum_{n=0}^{\infty} \frac{1}{n!}|z|^n |\nabla^n u(\mathbf{x})| \le C \left[\frac{1}{1-|z|/(cr)} + \exp(C'|z|/\varepsilon) \right].$$

for suitable C, C'. The analyticity of M on closure($\widetilde{G}$) implies the existence of $\delta > 0$ (independent of $\widetilde{\mathbf{x}} = (\widetilde{x}, \widetilde{y}) \in \widetilde{G}$) such that

$$M(\widetilde{x} + B_{\delta r}(0), \widetilde{y} + B_{\delta r}(0)) \subset B_{\frac{1}{2}cr(\mathbf{x})}(\mathbf{x}).$$

For $\alpha \in \mathbb{N}_0^2$ let $\theta := \min\{\delta r(\mathbf{x}), (|\alpha|+1)\varepsilon\}$. The Cauchy integral theorem for derivatives gives

$$\partial_{\widetilde{x}}^{\alpha_1} \partial_{\widetilde{y}}^{\alpha_2} \widetilde{u}(\widetilde{x}, \widetilde{y}) = -\frac{\alpha_1! \alpha_2!}{4\pi^2} \int_{z_1 \in \partial B_\theta(0)} \int_{z_2 \in \partial B_\theta(0)} \frac{\widetilde{u}(M(\widetilde{\mathbf{x}} + (z_1, z_2)))}{(-z_1)^{\alpha_1+1}(-z_2)^{\alpha_2+1}}$$

so that we get

$$\begin{aligned} |\partial_{\widetilde{x}}^{\alpha_1} \partial_{\widetilde{y}}^{\alpha_2} \widetilde{u}(\widetilde{x}, \widetilde{y})| &\lesssim \alpha_1! \alpha_2! \theta^{-|\alpha|} \left[1 + \exp(C'\theta/\varepsilon)\right] \\ &\lesssim |\alpha|! \max\{(\delta r(\mathbf{x}))^{-1}, (|\alpha|+1)^{-1}\varepsilon^{-1}\}^{|\alpha|} \left[1 + \exp(C'|\alpha|)\right], \end{aligned}$$

which proves the asserted estimate. ∎

Appendix B. Univariate Approximation.

LEMMA B.1. *Let $I = (-1, 1)$ and $u \in C^\infty(I)$ satisfy, for some constants C_u, $\gamma_u > 0$ and some $h \in (0, 1]$, $\varepsilon \in (0, 1]$ the bound*

$$\forall n \in \mathbb{N}_0 \colon \quad \|D^n u\|_{L^\infty(I)} \le C_u (\gamma_u h)^n \max\{n, \varepsilon^{-1}\}^n. \tag{B.1}$$

Then there are constants C, η, $\delta > 0$ depending solely on γ_u such that under the constraint

$$\frac{h}{\varepsilon q} \le \delta \tag{B.2}$$

there holds

$$\forall q \in \mathbb{N} \colon \quad \inf_{v \in \mathbb{P}_q} \|u - v\|_{W^{1,\infty}(I)} \le C C_u \left(\left(\frac{h}{h+\eta} \right)^{q+1} + \left(\frac{h}{\eta \varepsilon q} \right)^{q+1} \right). \tag{B.3}$$

Proof. We start with the observation that Taylor's theorem yields for $x > 0$

$$\sum_{n \ge q+1} \frac{1}{n!} x^n = e^x - \sum_{n=0}^{q} \frac{x^n}{n!} = \frac{1}{q!} \int_0^x (x-t)^q e^t \, dt \le \frac{x^{q+1}}{q!} e^x. \tag{B.4}$$

Case 1: Let $e\gamma_u h < 1/2$. Then the Taylor series of u about $x_0 = 0$ converges in I and the Taylor polyomials $T_q \in \mathbb{P}_q$ satisfy the error bounds

$$\begin{aligned} \|u - T_q\|_{L^\infty(I)} &\le \sum_{n=q+1}^{\infty} \frac{|D^n u(0)|}{n!} \le C_u \sum_{n=q+1}^{\infty} (\gamma_u e h)^n + \frac{(\gamma_u h/\varepsilon)^n}{n!} \\ &\overset{(B.4)}{\le} C_u \left(\frac{(\gamma_u e h)^{q+1}}{1 - (\gamma_u e h)} + \frac{(\gamma_u h/\varepsilon)^{q+1}}{q!} e^{\gamma_u h/\varepsilon} \right) \\ &\overset{(B.8)}{\le} C_u \left(2(\gamma_u e h)^{q+1} + C(\gamma' h/(\varepsilon q))^{q+1} e^{\gamma_u h/\varepsilon} \right), \end{aligned}$$

for suitable $\gamma' > \gamma_u$. The assumption (B.2) allows us to estimate $e^{\gamma_u h/\varepsilon} \le e^{\gamma_u \delta q}$ and the desired result follows for the L^∞-estimate. An analogous argument applies for the $W^{1,\infty}$-estimate.

Case 2: Let $1 \ge h > 1/(2e\gamma_u)$. Introduce for $\rho > 1$ the ellipse $\mathcal{E}_\rho := \{z \in \mathbb{C} \,|\, |z-1|+|z+1| < \rho+1/\rho\}$ and set $G_\kappa(I) := \cup_{x\in I} B_\kappa(x)$. By geometric considerations (e.g., with the aid of [7, Lemma 3.14]) one has $\mathcal{E}_{1+\kappa} \subset G_\kappa(I)$. Taylor's theorem gives that u is holomorphic on $G_{1/(\gamma_u h)}(I)$ and for every $\kappa < 1/(\gamma_u h)$ we have

(B.5)
$$\|u\|_{L^\infty(G_\kappa)} \le C_u \sum_{n=0}^{\infty} \frac{1}{n!} (h\gamma_u\kappa)^n \max\{n, \varepsilon^{-1}\}^n \le C_u \left[\frac{1}{1 - e\gamma_u h\kappa} + \exp(\kappa\gamma_u h/\varepsilon) \right].$$

Well-established polynomial approximation results (see, e.g., [1, Thm. 6]) then yield for fixed $\kappa > 0$ the existence of $\rho_1 = \rho_1(\kappa) > 1$ such that

$$\inf_{v\in\mathbb{P}_q} \|u - v\|_{W^{1,\infty}(I)} \le CC_u\rho_1^{-q}\|u\|_{L^\infty(G_\kappa)} \le CC_u\rho_1^{-q}e^{\kappa\gamma_u h/\varepsilon} \le CC_u\rho_1^{-q}e^{\kappa\gamma_u\delta q}.$$

Fix $1 < \rho_2 < \rho_1$. Then we may select $\delta > 0$ sufficiently small so that there exists a constant $C > 0$ such that

$$\forall q \in \mathbb{N}: \quad \inf_{v\in\mathbb{P}_q} \|u - v\|_{W^{1,\infty}(I)} \le CC_u\rho_2^{-q}.$$

Using $h \ge 1/(2e\gamma_u)$ and suitably choosing η, we can estimate

$$\rho_2^{-q} \le \left(\frac{h}{h+\eta}\right)^q. \qquad \square$$

Lemma B.2 (stability of the 1d-Gauss-Lobatto (GL) interpolant). *Let $I = [-1, 1]$. There exists a constant $C > 0$ such that for any $q \in \mathbb{N}$, the Gauss-Lobatto interpolation operator $i_q : C(I) \to \mathbb{P}_q$ satisfies:*

$$\|u - i_q u\|_{L^\infty(I)} \le (1 + \Lambda_q) \inf_{v\in\mathbb{P}_q} \|u - v\|_{L^\infty(I)}, \qquad \Lambda_q = C\ln(q + 1), \tag{B.6}$$

$$\|(u - i_q u)'\|_{L^\infty(I)} \le C(1 + q^2\Lambda_q) \inf_{v\in\mathbb{P}_q} \|(u - v)'\|_{L^\infty(I)}. \tag{B.7}$$

Proof. The bound (B.6) follows from the projection property of the Gauss-Lobatto interpolation; the logarithmic growth of the Lebesgue constant Λ_q is shown in [33].

For (B.7), we estimate for arbitrary $v \in \mathbb{P}_q$

$$\begin{aligned}\|(u - i_q u)'\|_{L^\infty(I)} &\le \|(u - v)'\|_{L^\infty(I)} + \|(i_q(u - v))'\|_{L^\infty(I)} \\ &\lesssim \|(u - v)'\|_{L^\infty(I)} + q^2\|i_q(u - v)\|_{L^\infty(I)} \lesssim \|(u - v)'\|_{L^\infty(I)} + q^2\Lambda_q\|u - v\|_{L^\infty(I)}.\end{aligned}$$

Constraining v to satisfy $v(-1) = u(-1)$ the result follows from a Poincaré inequality. $\square$

Finally, we recall two inequalities of Stirling's type.

$$\forall n \in \mathbb{N}: \quad \sqrt{2\pi}n^{n+1/2}e^{-n} \le n! \le en^{n+1/2}e^{-n}\ , \tag{B.8}$$

$$\forall n \in \mathbb{N}_0 \quad \forall \alpha \in \mathbb{N}_0: \quad \alpha!n! \ge 2^{-(\alpha+n)}(\alpha + n)! \ge (2e)^{-(\alpha+n)}(\alpha + n)^{\alpha+n}. \tag{B.9}$$

(B.8) follows from [22]. In B.9, the first bound follows from the binomial formula $\sum_{\nu=0}^{m} \binom{m}{\nu} x^\nu = (1 + x)^m$ and the second bound follows from (B.8).

REFERENCES

[1] T. Apel and J.M. Melenk. Interpolation and quasi-interpolation in *h*- and *hp*-version finite element spaces. In E. Stein, R. de Borst, and T.J.R. Hughes, editors, Encyclopedia of Computational Mechanics, pages 1–33. John Wiley & Sons, Chichester, UK, second edition, 2018. extended preprint at `http://www.asc.tuwien.ac.at/preprint/2015/asc39x2015.pdf`.

[2] Douglas N. Arnold and Richard S. Falk. Asymptotic analysis of the boundary layer for the Reissner-Mindlin plate model. SIAM J. Math. Anal., 27(2):486–514, 1996.

[3] I. Babuška and B.Q. Guo. The $h-p$ version of the finite element method. Part 1: The basic approximation results. Computational Mechanics, 1:21–41, 1986.

[4] I. Babuška and B.Q. Guo. The $h-p$ version of the finite element method. Part 2: General results and applications. Computational Mechanics, 1:203–220, 1986.

[5] I. Babuška and B.Q. Guo. The *h*-*p* version of the finite element method for domains with curved boundaries. SIAM J. Numer. Anal., 25(4):837–861, 1988.

[6] Lehel Banjai, Jens M. Melenk, Ricardo H. Nochetto, Enrique Otarola, Abner J. Salgado, and Christoph Schwab. Tensor FEM for spectral fractional diffusion. Journ. Found. Comp. Math., 2018.

[7] Steffen Börm, Maike Löhndorf, and Jens M. Melenk. Approximation of integral operators by variable-order interpolation. Numer. Math., 99(4):605–643, 2005.

[8] François Buret, Monique Dauge, Patrick Dular, Laurent Krähenbühl, Victor Péron, Ronan Perrussel, Clair Poignard, and Damien Voyer. Eddy cur-rents and corner singularities. IEEE Transactions on Magnetics, 48(2):679–68, 2012.

[9] Marie Chaussade-Beaudouin, Monique Dauge, Erwan Faou, and Zohar Yosibash. Free vibrations of axisymmetric shells: parabolic and elliptic cases. Asymptot. Anal., 104(1-2):1–47, 2017.

[10] Leszek Demkowicz, Jay Gopalakrishnan, and Antti H. Niemi. A class of discontinuous Petrov-Galerkin methods. Part III: Adaptivity. Appl. Numer. Math., 62(4):396–427, 2012.

[11] M. Faustmann and J. M. Melenk. Robust exponential convergence of *hp*-FEM in balanced norms for singularly perturbed reaction-diffusion problems: corner domains. Comput. Math. Appl., 74(7):1576–1589, 2017.

[12] K. Gerdes, A. M. Matache, and C. Schwab. Analysis of membrane locking in *hp* FEM for a cylindrical shell. ZAMM Z. Angew. Math. Mech., 78(10):663–686, 1998.

[13] Gung-Min Gie, Makram Hamouda, Chang-Yeol Jung, and Roger M. Temam. Singular perturbations and boundary layers, volume 200 of Applied Mathematical Sciences. Springer, Cham, 2018.

[14] J. M. Melenk and S. Sauter. Convergence analysis for finite element discretizations of the Helmholtz equation with Dirichlet-to-Neumann boundary conditions. Math. Comp., 79(272):1871–1914, 2010.

[15] Jens Melenk. A note on robust exponential convergence of finite element methods for problems with boundary layers. IMA Journal of Numerical Analysis, 17:557–601, 1997.

[16] Jens Melenk and Christoph Schwab. An *hp* finite element method for convection-diffusion problems in one dimension. IMA Journal of Numerical Analysis, 19(3):425–453, 1999.

[17] Jens Markus Melenk and Alexander Rieder. *hp*-FEM for the fractional heat equation, 2019. 1901.01767.

[18] J.M. Melenk. *hp*-finite element methods for singular perturbations, volume 1796 of Lecture Notes in Mathematics. Springer-Verlag, Berlin, 2002.

[19] J.M. Melenk and Ch. Schwab. *hp* FEM for reaction-diffusion equations. I. Robust exponential convergence. SIAM J. Numer. Anal., 35(4):1520–1557, 1998.

[20] J.M. Melenk and Ch. Schwab. Analytic regularity for a singularly perturbed problem. SIAM J. Math. Anal., 30(2):379–400, 1999.

[21] J. J. H. Miller, E. O'Riordan, and G. I. Shishkin. Fitted numerical methods for singular perturbation problems. World Scientific Publishing Co., Inc., River Edge, NJ, 1996. Error estimates in the maximum norm for linear problems in one and two dimensions.

[22] Herbert Robbins. A remark on Stirling's formula. Amer. Math. Monthly, 62:26–29, 1955.

[23] Hans-Görg Roos, Martin Stynes, and Lutz Tobiska. Robust numerical methods for singularly perturbed differential equations, volume 24 of Springer Series in Computational Mathematics. Springer-Verlag, Berlin, second edition, 2008. Convection-diffusion-reaction and flow problems.

[24] J. Schöberl. Netgen an advancing front 2d/3d-mesh generator based on abstract rules. J. Comput. Visual. Sci., 1:41–52, 1997.

[25] Dominik Schötzau and Christoph Schwab. Exponential convergence for hp-version and spectral

finite element methods for elliptic problems in polyhedra. M3AS, 25(9):1617–1661, 2015.

[26] Dominik Schötzau and Christoph Schwab. Exponential convergence of *hp*-FEM for elliptic problems in polyhedra: Mixed boundary conditions and anisotropic polynomial degrees. Journ. Found. Comput. Math., 18(3):595–660, 2018.

[27] Dominik Schötzau, Christoph Schwab, and Rolf Stenberg. Mixed *hp*-FEM on anisotropic meshes. II. Hanging nodes and tensor products of boundary layer meshes. Numer. Math., 83(4):667–697, 1999.

[28] Dominik Schötzau, Christoph Schwab, and Thomas Wihler. *hp*-DGFEM for Second-Order Elliptic Problems in Polyhedra II: Exponential Convergence. SIAM J. Numer. Anal., 51(4):2005–2035, 2013.

[29] Ch. Schwab. *p*- and *hp*-Finite Element Methods. Numerical Mathematics and Scientific Computation. The Clarendon Press, Oxford University Press, New York, 1998. Theory and applications in solid and fluid mechanics.

[30] Ch. Schwab, M. Suri, and C. Xenophontos. The *hp* finite element method for problems in mechanics with boundary layers. Comput. Methods Appl. Mech. Engrg., 157(3-4):311–333, 1998. Seventh Conference on Numerical Methods and Computational Mechanics in Science and Engineering (NMCM 96) (Miskolc).

[31] Ch. Schwab, M. Suri, and C.A. Xenophontos. The *hp* Finite Element Method for problems in mechanics with boundary layers. Comp. Meth. Appl. Mech. Engg., 157(3-4):311–333, 1998.

[32] G. I. Shishkin. Approximation of solutions of singularly perturbed boundary value problems with a corner boundary layer. Zh. Vychisl. Mat. i Mat. Fiz., 27(9):1360–1374, 1438, 1987.

[33] B. Sündermann. Lebesgue constants in Lagrangian interpolation at the Fekete points. Mitt. Math. Ges. Hamb., 11:204–211, 1983.